

Inside the XPS

Advanced Solid State & Surface Characterization

Pascal Schouwink
Mounir Mensi
Emad Oveisi

2025/03/26

Course 7: Plan

- ❖ Sample preparation and surface contamination
- ❖ Depth profiling
- ❖ Chemical Analysis
 - ❖ Origins of the 'chemical shift'
 - ❖ Magnitude of the 'chemical shift'
- ❖ Quantification
 - ❖ Concepts
 - ❖ Example
- ❖ Dedicated Techniques
 - ❖ XPS Mapping
 - ❖ ARXPS
 - ❖ Ag La High Energy XPS

Preparing and Mounting the Sample

In the majority of XPS applications, sample preparation and mounting are not critical. However, to ensure a clean working sample, several conditions have to meet. Aside from volatile material which are naturally out gazing under the UHV present in the analysis chamber.

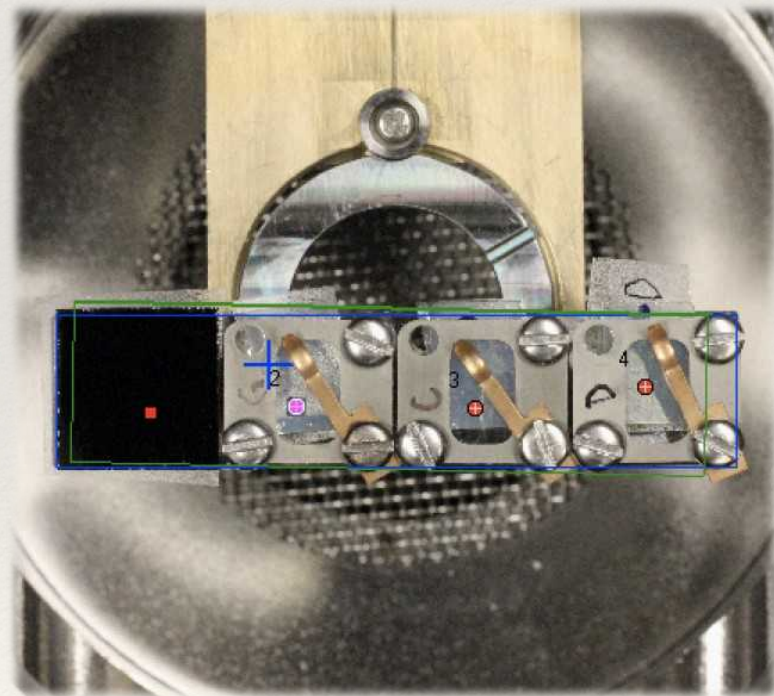
- ❖ Abrasion (e.g. elimination of an oxide layer)
- ❖ Sputter etching (e.g. removal of organic contaminants)
- ❖ Fracturing (e.g. reveals a fresh surface)
- ❖ Ground to powders (mounted onto a vacuum compatible tape)

So...what can go wrong?

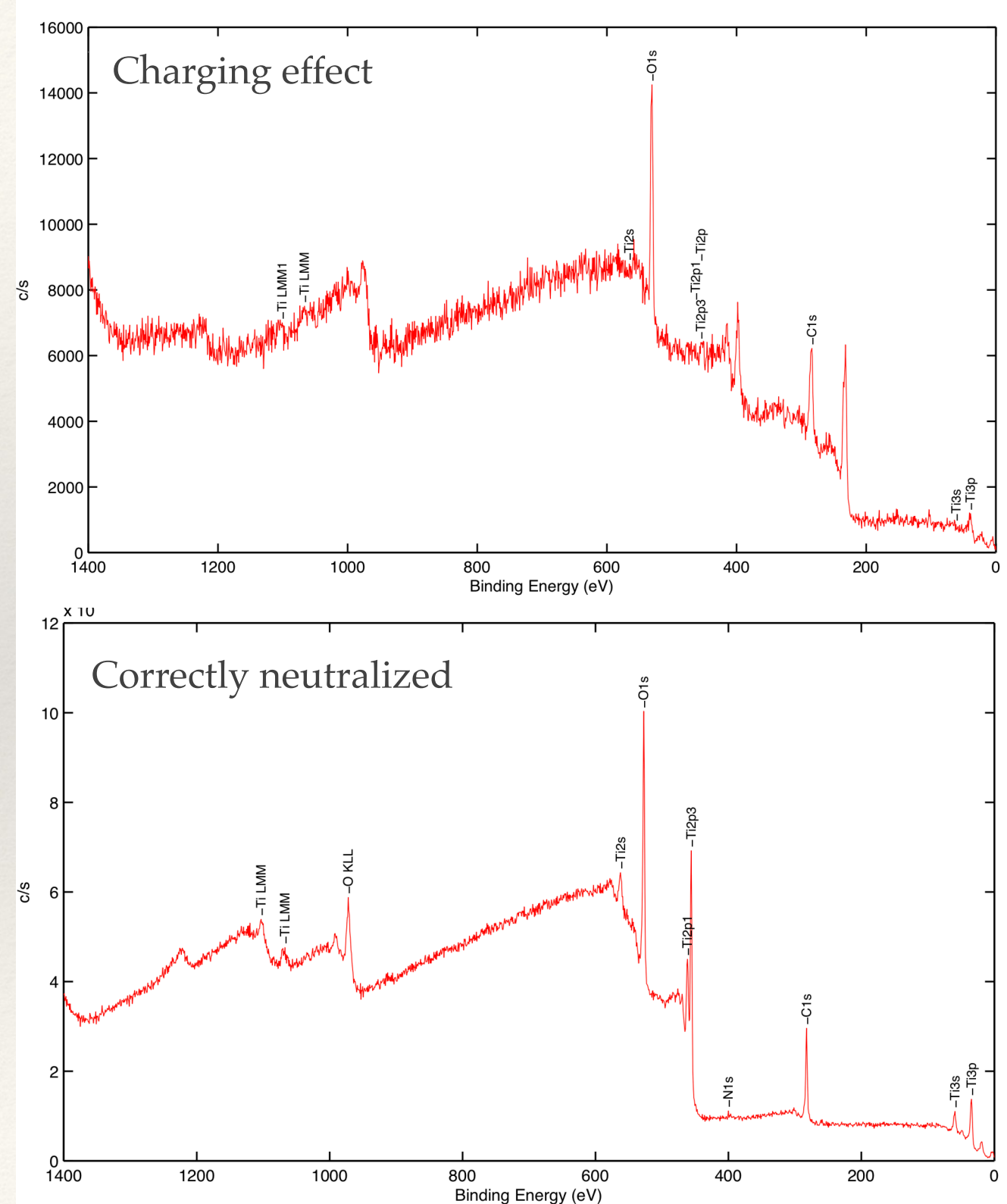
Mounting Insulating Samples

For dielectric samples, care has to be taken to avoid sample charging. Build up of charges at the surface might deform the spectra through

- ❖ Peak broadening
- ❖ Peak deformation



The samples are grounded, however, insulating sample exhibit some strong charging effects

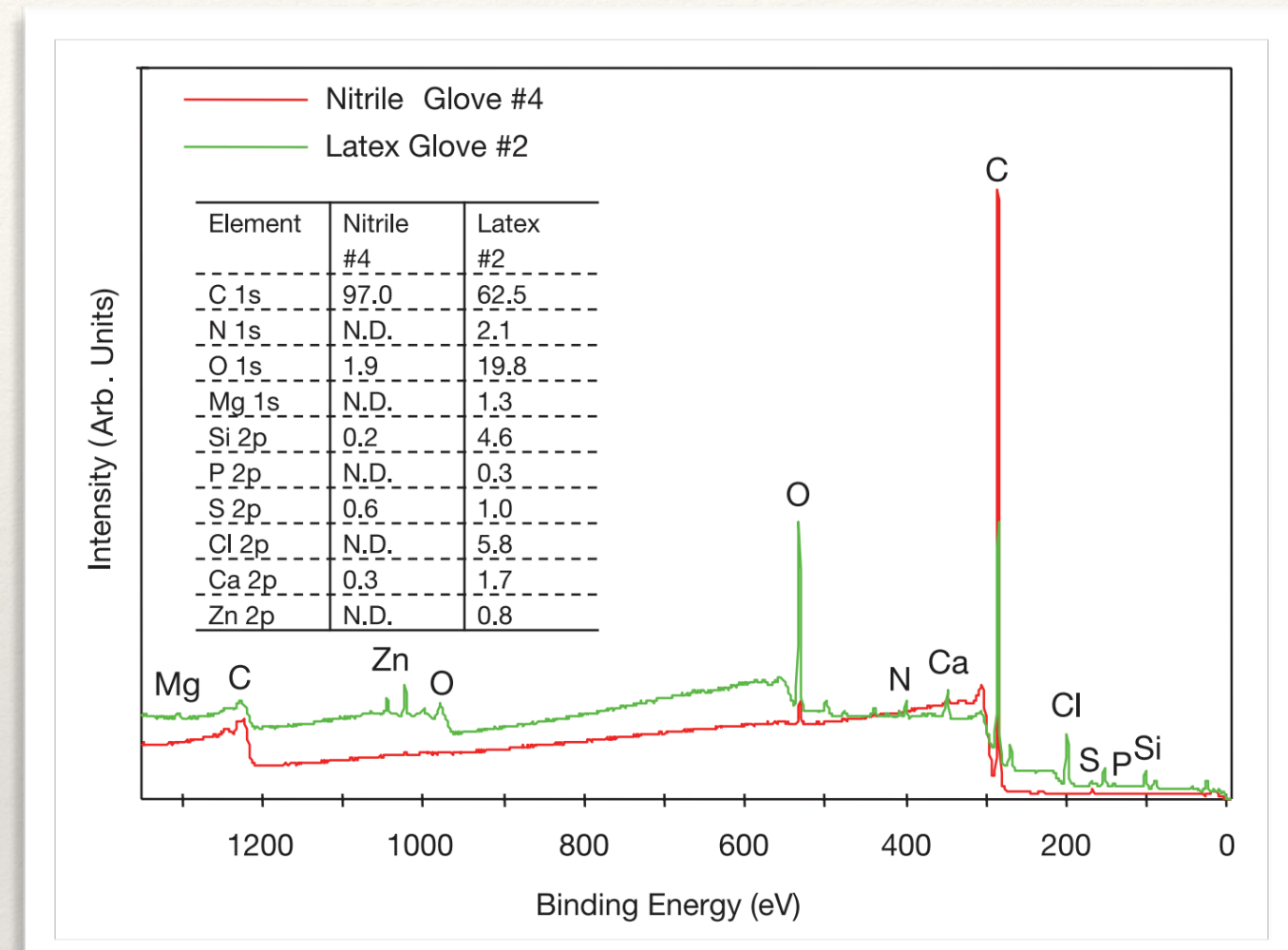


Study Case I: Clean Gloves?

15 different pairs of lab gloves have been measured by XPS. The results show that the surfaces composition can vary to a large degree.

Nitrile glove had only a small amount of oxygen present plus a few minor surface components (e.g., Si, S, and Ca).

Latex glove had much lower carbon and approximately ten times the oxygen present along with significant amounts of N, Mg, Si, S, Cl, and Ca, plus minor amounts of P and Zn.



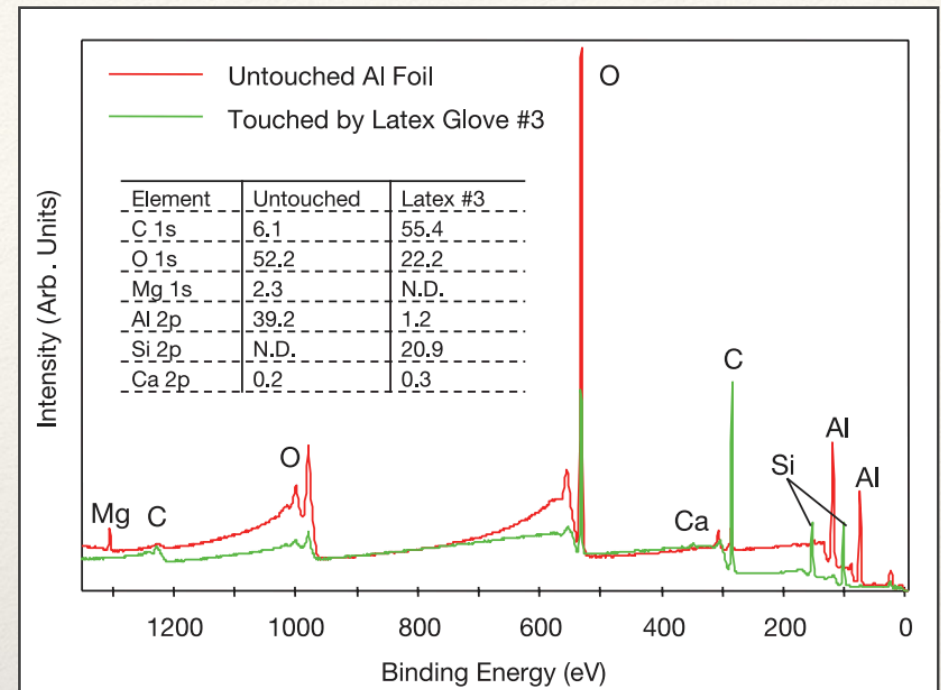
XPS survey spectra of the outer surfaces of nitrile and latex gloves and quantitative (atomic %) results

Study Case I: Cross Contamination

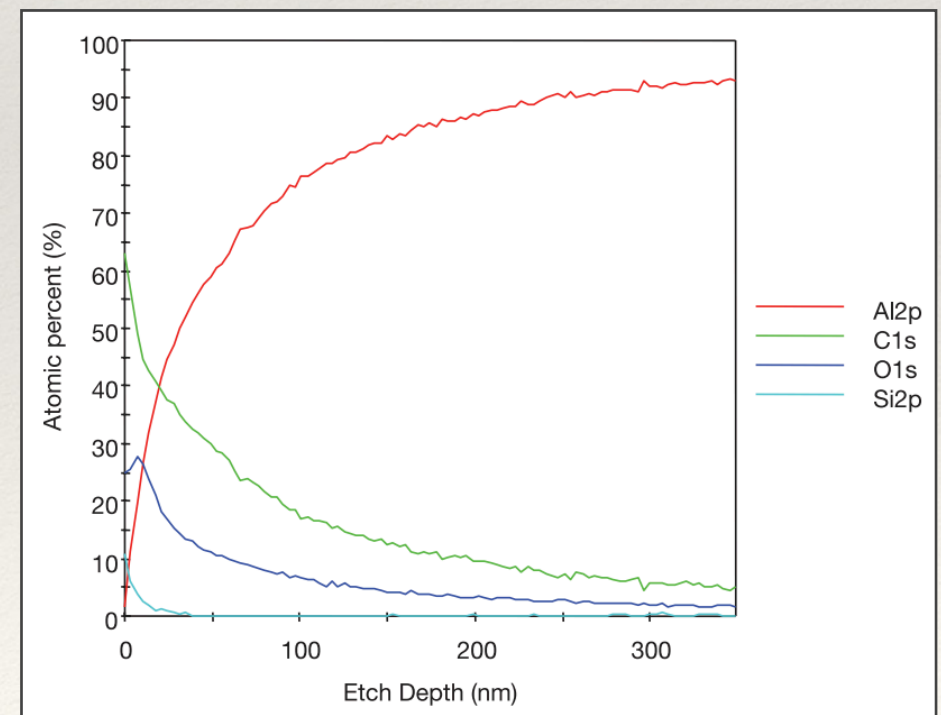
What happens under contact between the gloves and a sample surface is much more interesting:

- ❖ The sample is covered by carbon!
- ❖ Additional contaminants are presents

When handling surface for surface analysis or where surface cleanliness is a priority, **clean** handling tools should be used. Never gloves



Survey spectra

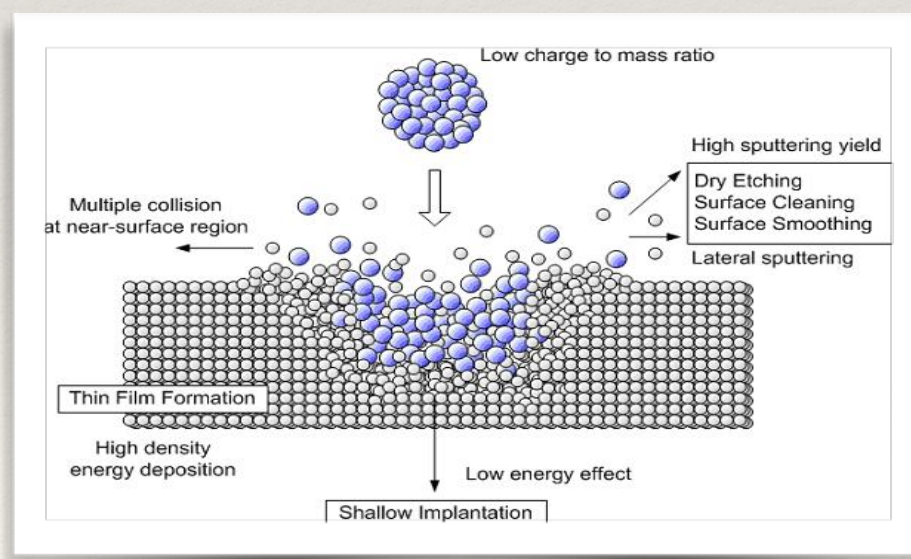


Depth Profile

Surface Contamination

When handling surface for surface analysis, where surface cleanliness is a priority, **clean handling tools should be used.**
Never gloves.

But ok...the contaminant is there...so let's try to remove it!



Sputter tests on contaminated sample

- ❖ Use of an Ar^+ sputtering
- ❖ Argon ion cluster sputtering



Copper Mine

Beneath the Surface

Ar+ and GCIB for

- Surface cleaning
- Depth Profiling

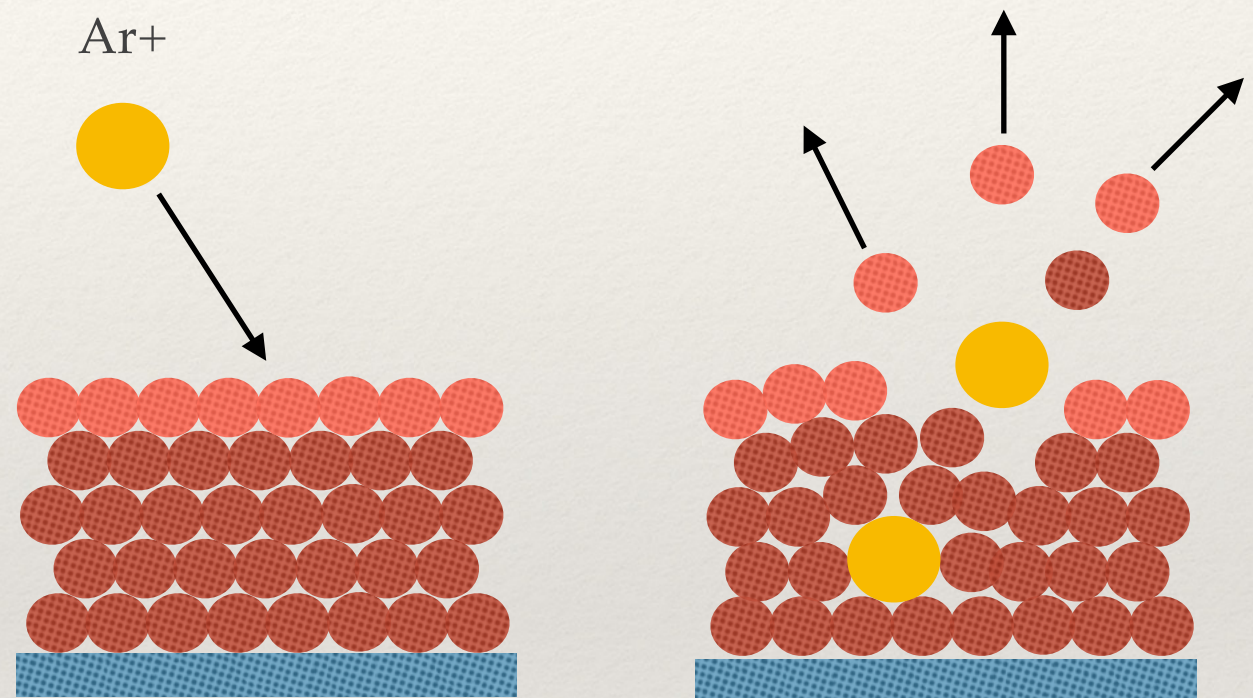
Surface Sputtering

Now that we have surface contaminated samples, either by adventitious atmospheric contamination (Ad.C.), surface adsorption or simply by mismanipulation, what can we do?

- ❖ Sputter clean the surface: Argon ion / Gas cluster ion beam sputtering. But ion sputtering offers much more than surface cleaning!
- ❖ Measure beneath the surface: High energy XPS and ARXPS (next course)

Argon Ion Sputtering Principle

Argon ions are accelerated (typically 0.1– 10 keV), towards the surface of the sample, efficiently sputtering the surface, removing contamination, but also creating damages on the surface.

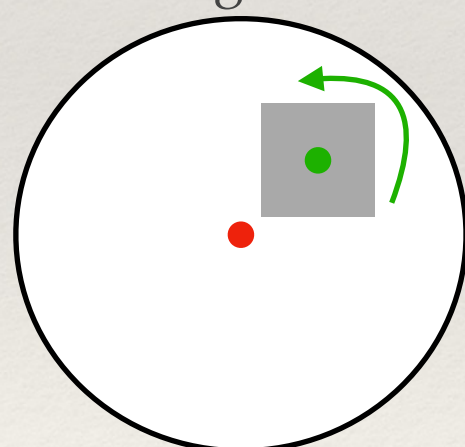


Sputtering, surface cleaning...and damages

Surface Cleaning Limitations

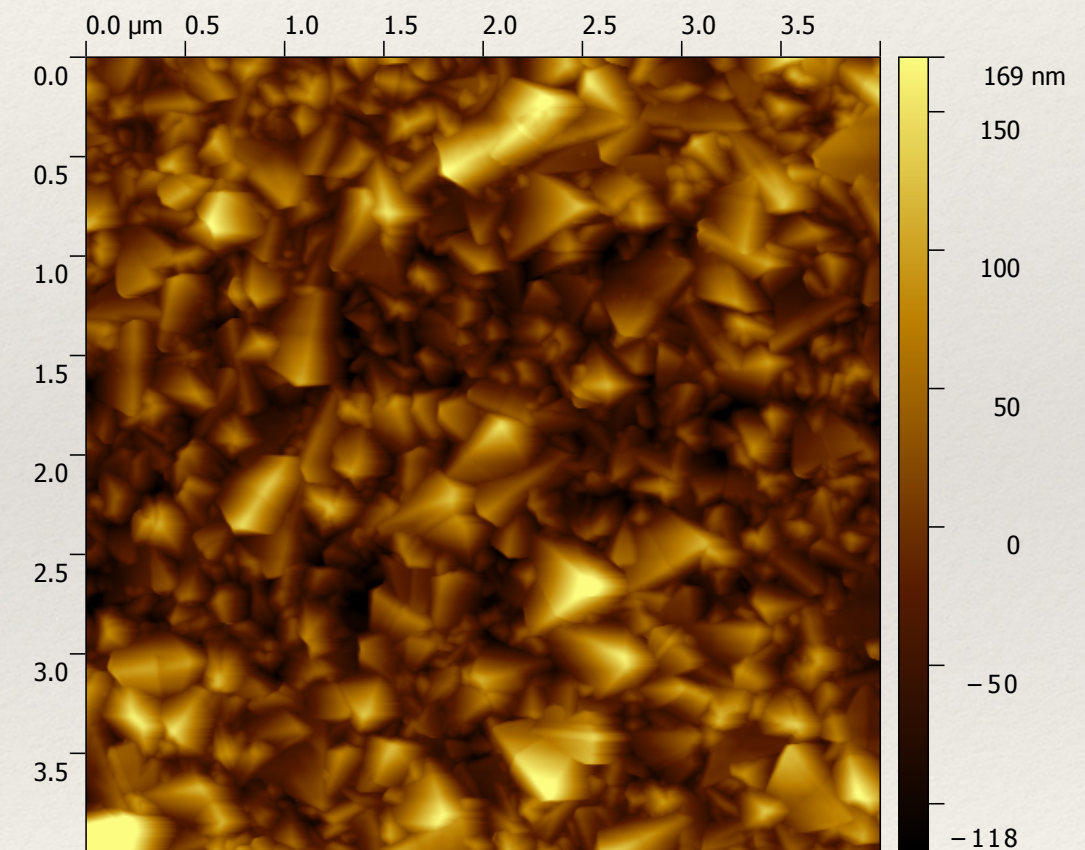
The efficiency and feasibility of organic contaminants removal largely depends on:

- ❖ The sample material: Organic contaminants could be easily cleaned-out from metallic surfaces leaving the main material virtually undamaged (through reconstruction)
- ❖ The sample topography / structure: Sharp angles prevent the ion beam to efficiently sputter the whole sample surface, due to **shadowing** effect. Compucentric/Zalar rotation might be use.



Rotation axis intersects
The sputter spot,
and not the center
of the sample stage

Schematics of a
compucentric rotation

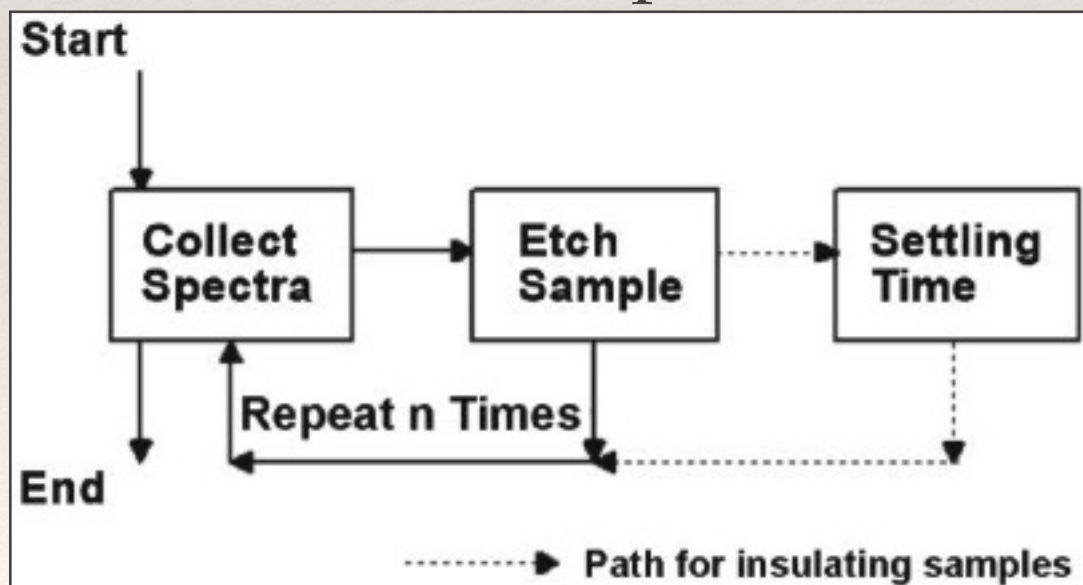


Topography of a typical FTO surface. Due to the surface roughness, ion sputtering would prove relatively inefficient

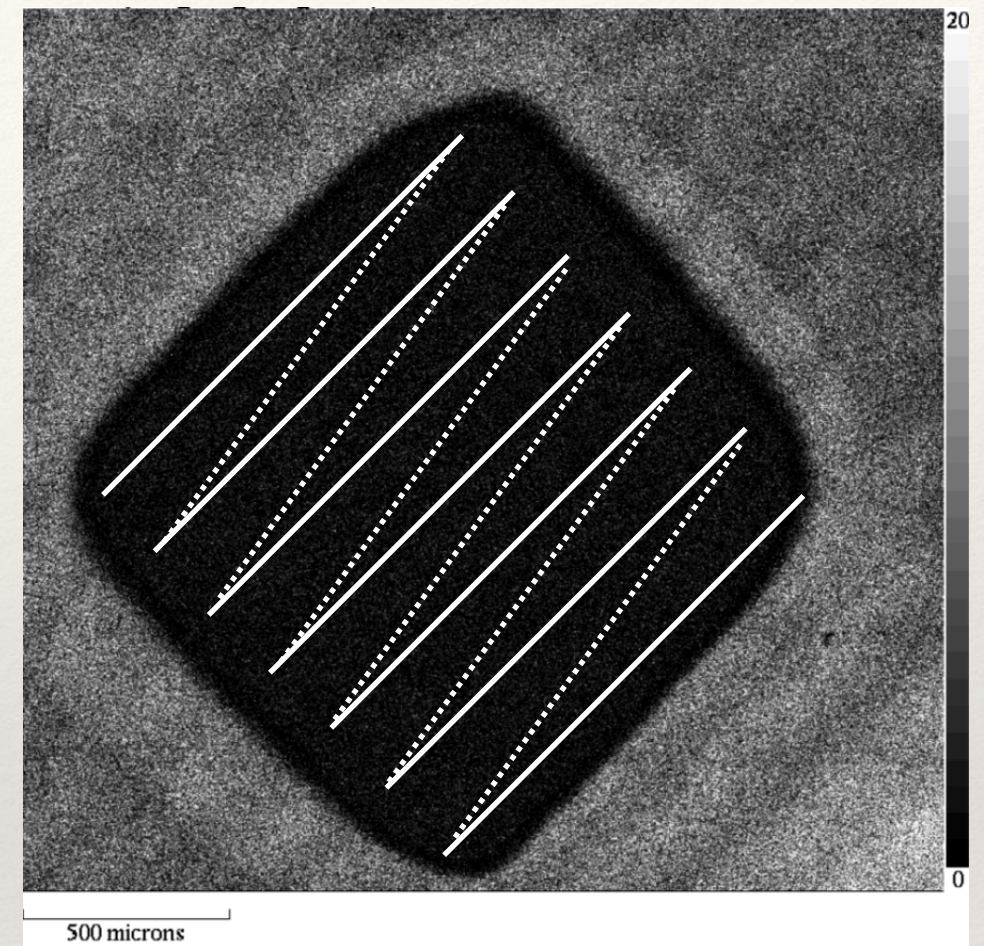
Depth Profiling

Depth profile is acquired using experimental loop (Zalar rotation possible):

1. A spectra is collected (survey or multiplex)
2. The surface is sputtered



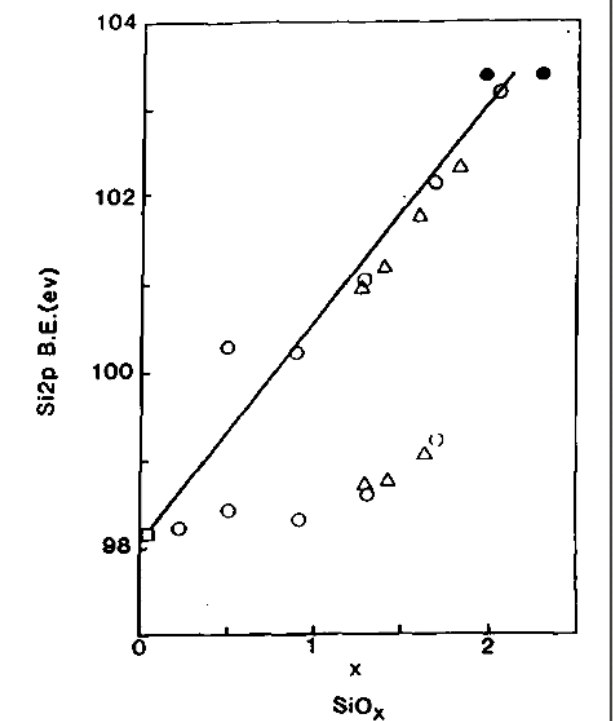
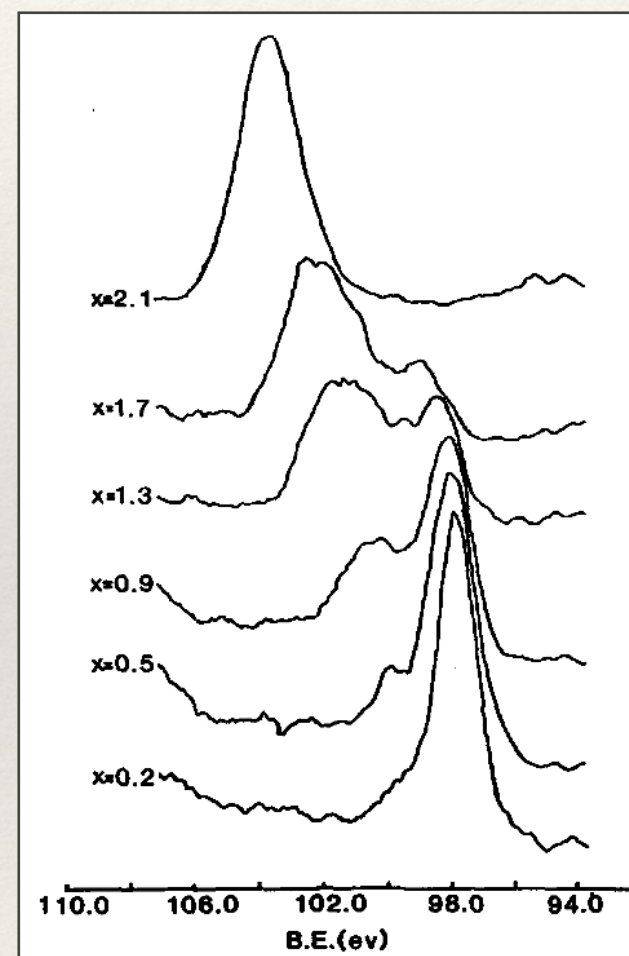
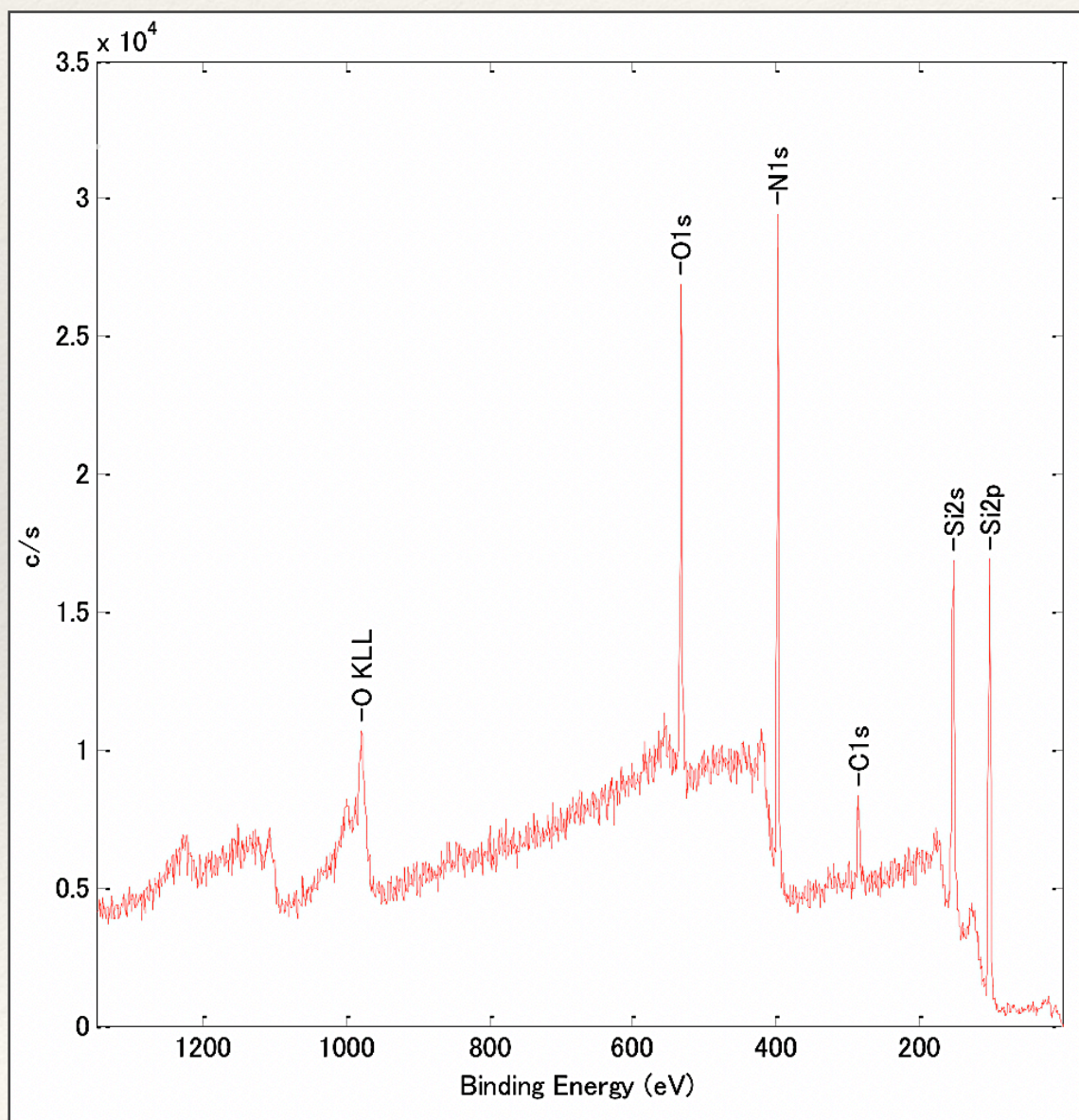
Typical cycle used for depth profiling



The ion beam is typically focused to a spot of 100μm, and raster scanned, creating a sharp edge created

Si₃N₄ on Si

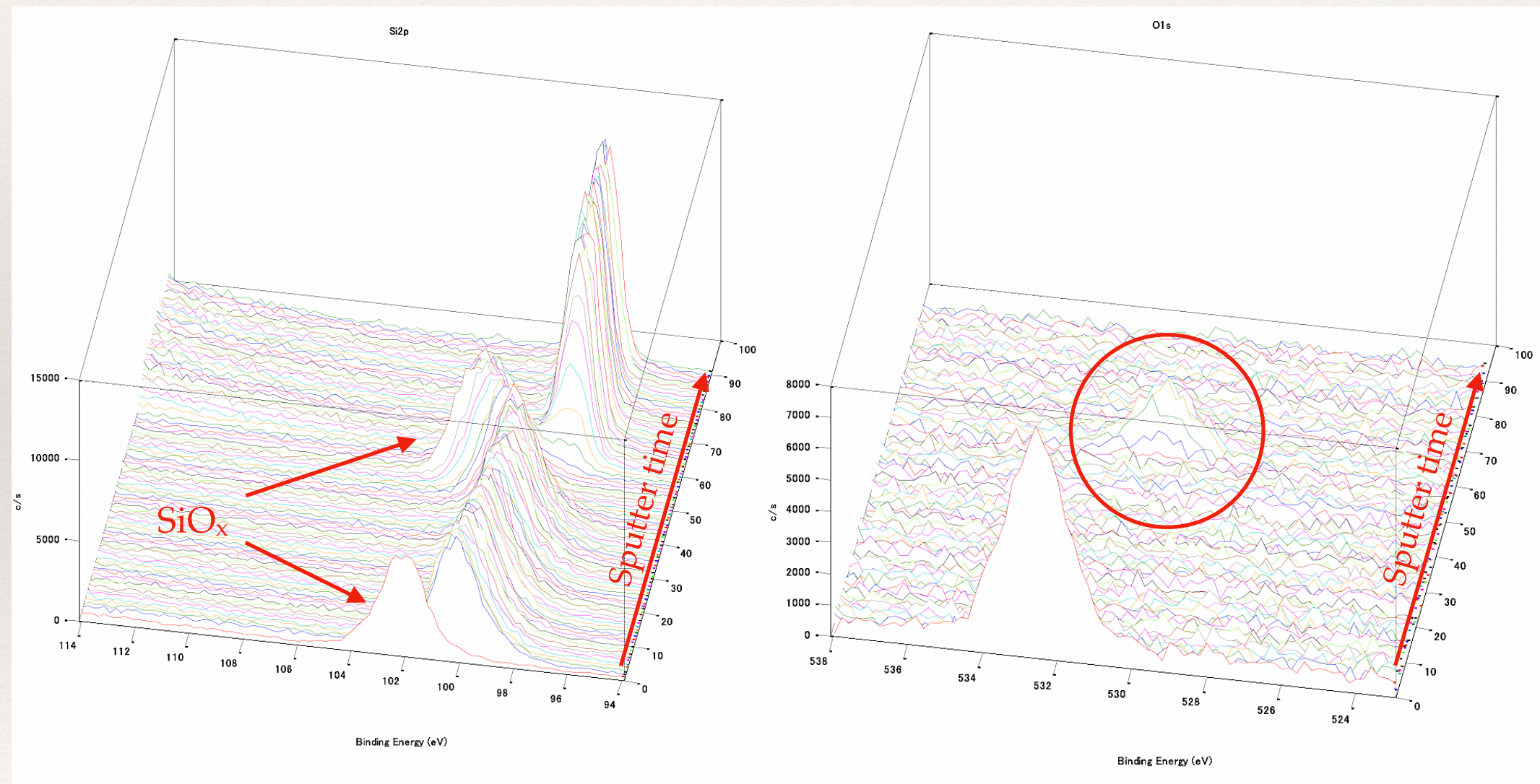
Surface properties: the top surface presents C, O, N and Si. A detailed analysis of the binding energy of Si, shows some SiO_x, which is could be explained by surface modification after the deposition



Y. N. SUN et al. X-Ray photoelectron spectroscopy of O_{1s} and Si_{2p} lines in films of SiO_x formed by electron beam evaporation. Thin Solid Films, 157 (1988) 351-360

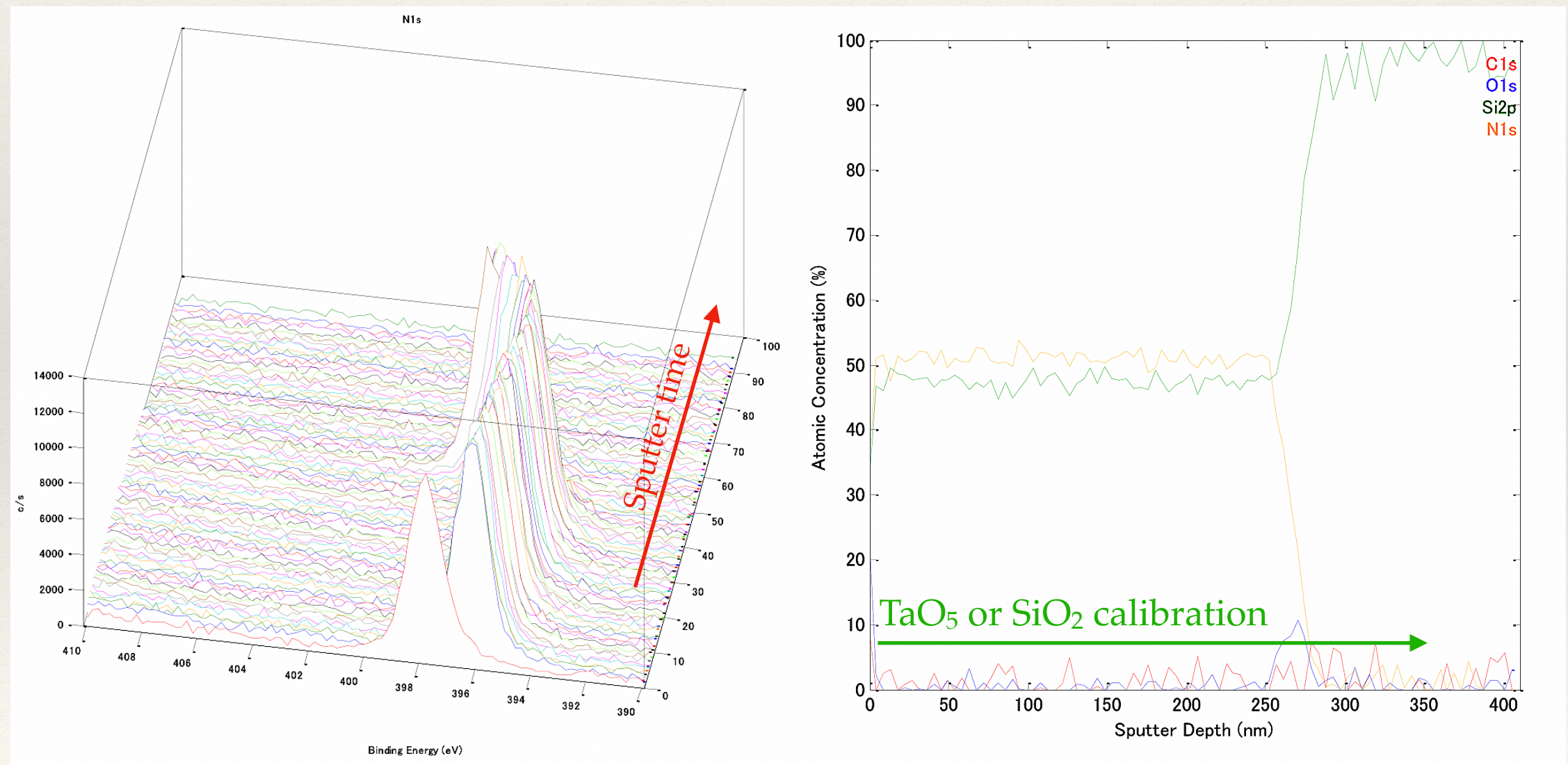
Si₃N₄ on Si: Depth Profiling

- ❖ The depth profile shows an excess of oxygen at ~60min of sputtering, along with a strong shift in the BE position of the Si 2p line, revealing an SiO_x interfacial layer



Si₃N₄ on Si: Depth Profiling

- ❖ Concomitantly, the N1s line presents similar features (left)
- ❖ Integrating the peak area, the depth profile plot is traced (right). It presents the relative surface atomic concentration of each element from the surface to the sputtered depth



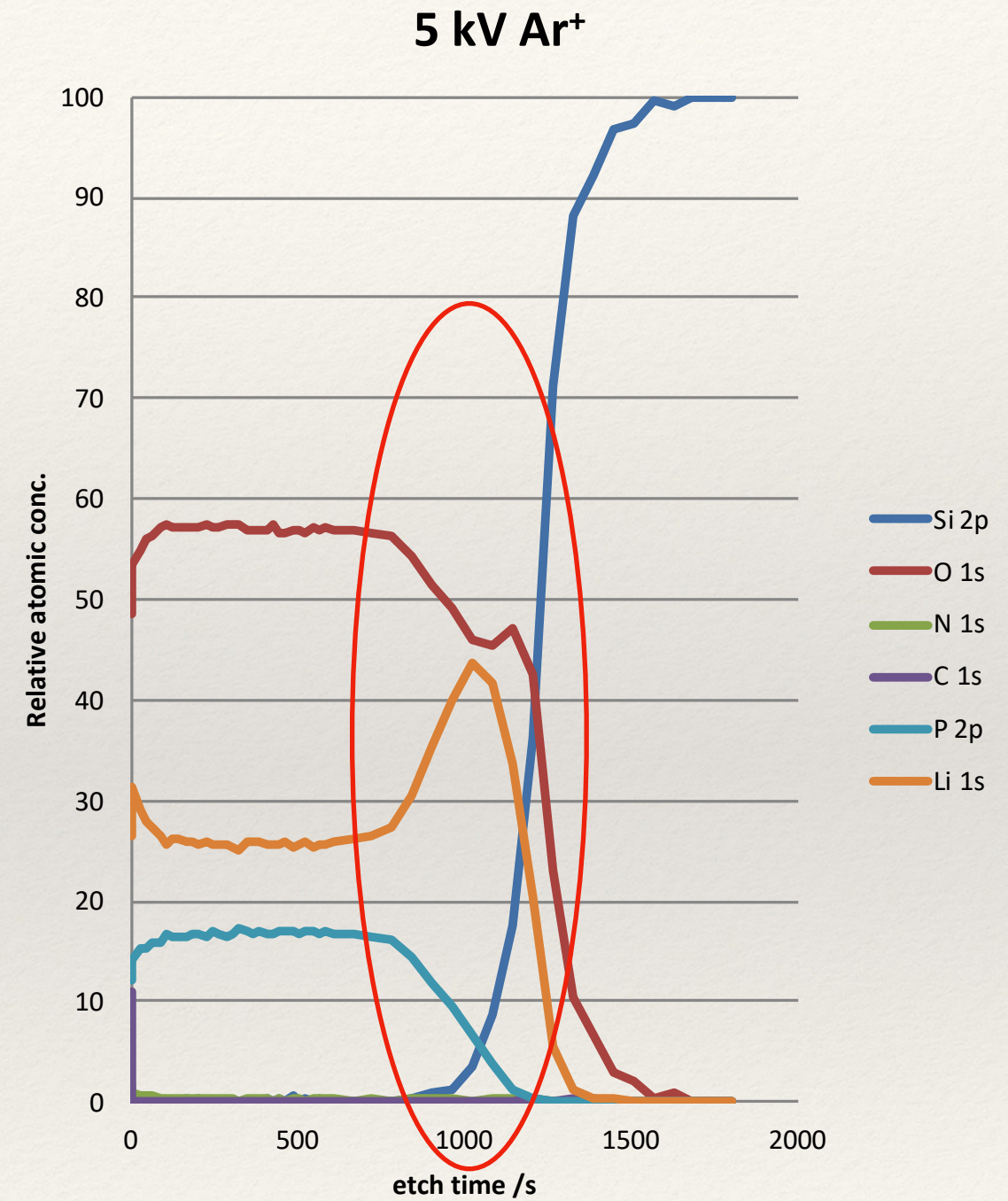
N1s line

Depth profile at%

Depth Profile: Implantation and Migration

Conventional monatomic depth profiling is susceptible to produce spurious results regarding both elemental concentration and chemical state identification as it triggers:

- ❖ Differential sputtering
- ❖ Implantation
- ❖ Migration
- ❖ Chemical modification



Migration of Li under the sputter.
The chemistry is also affected

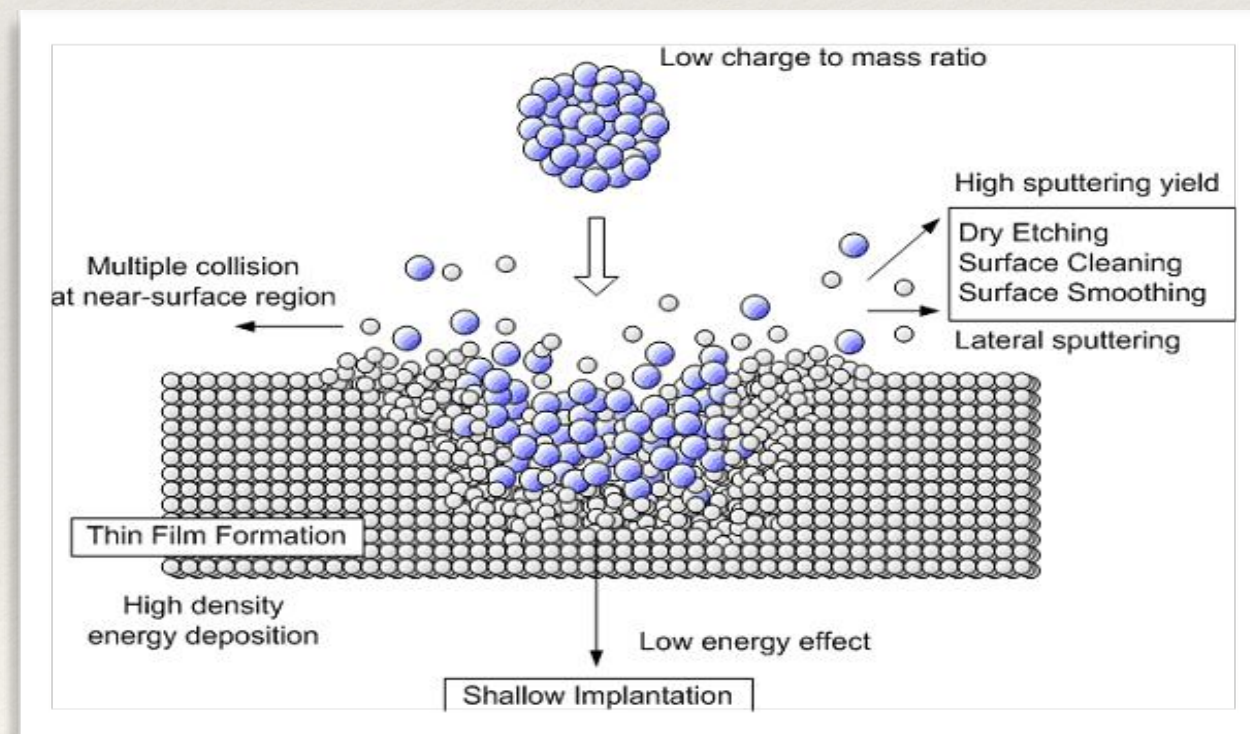
Argon Cluster Sputter Gun

Large clusters up to 5000 atoms are created and accelerated towards the surface with energy \sim 0.2-20keV

Low energy clusters are inefficient in sputtering inorganic material, i.e. ideal for surface cleaning

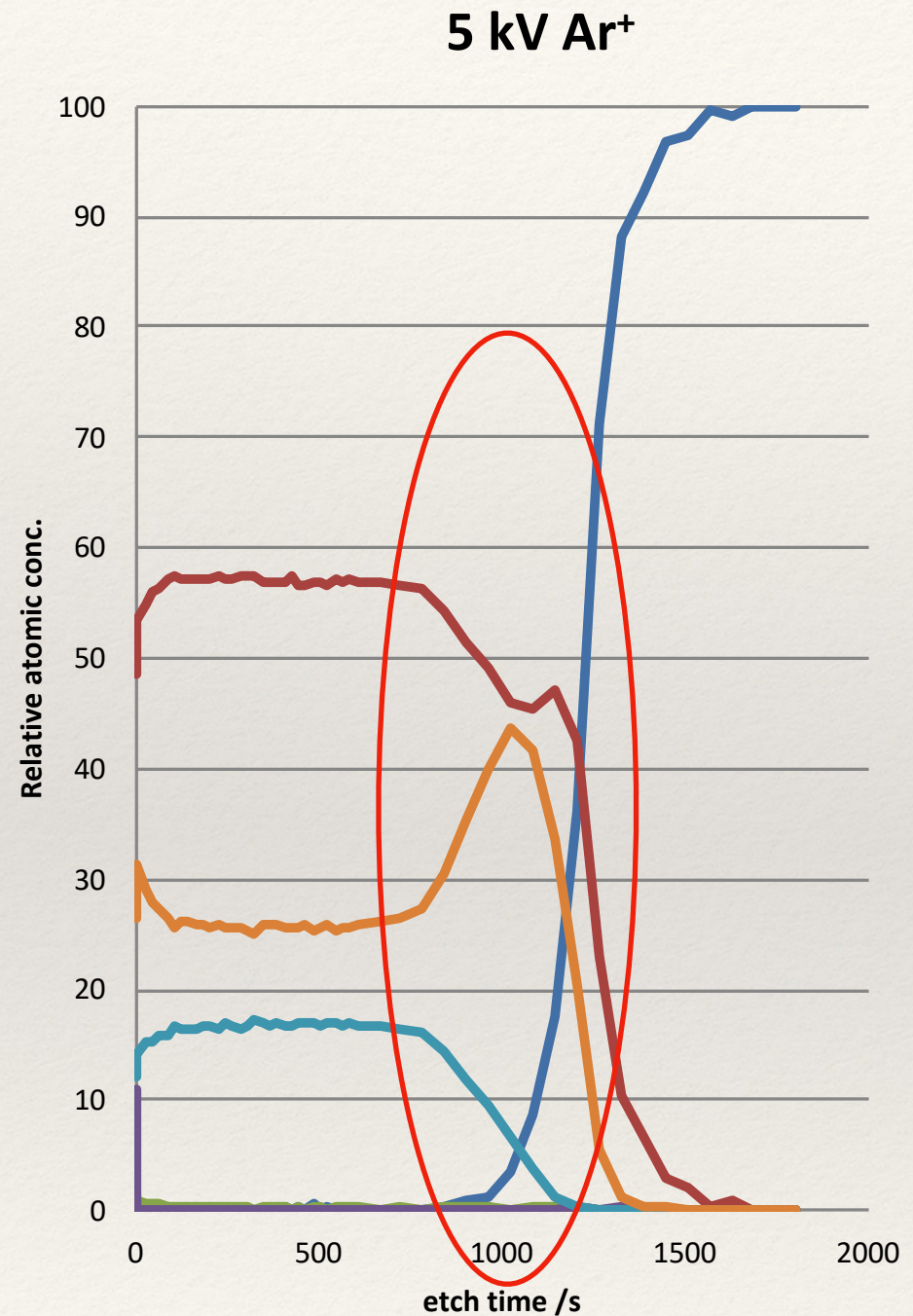
High energy cluster have a reasonable sputter rate for both organics and inorganic and allow:

- ❖ Reduction in light ion mobility
- ❖ Greater confidence in chemical state assignment

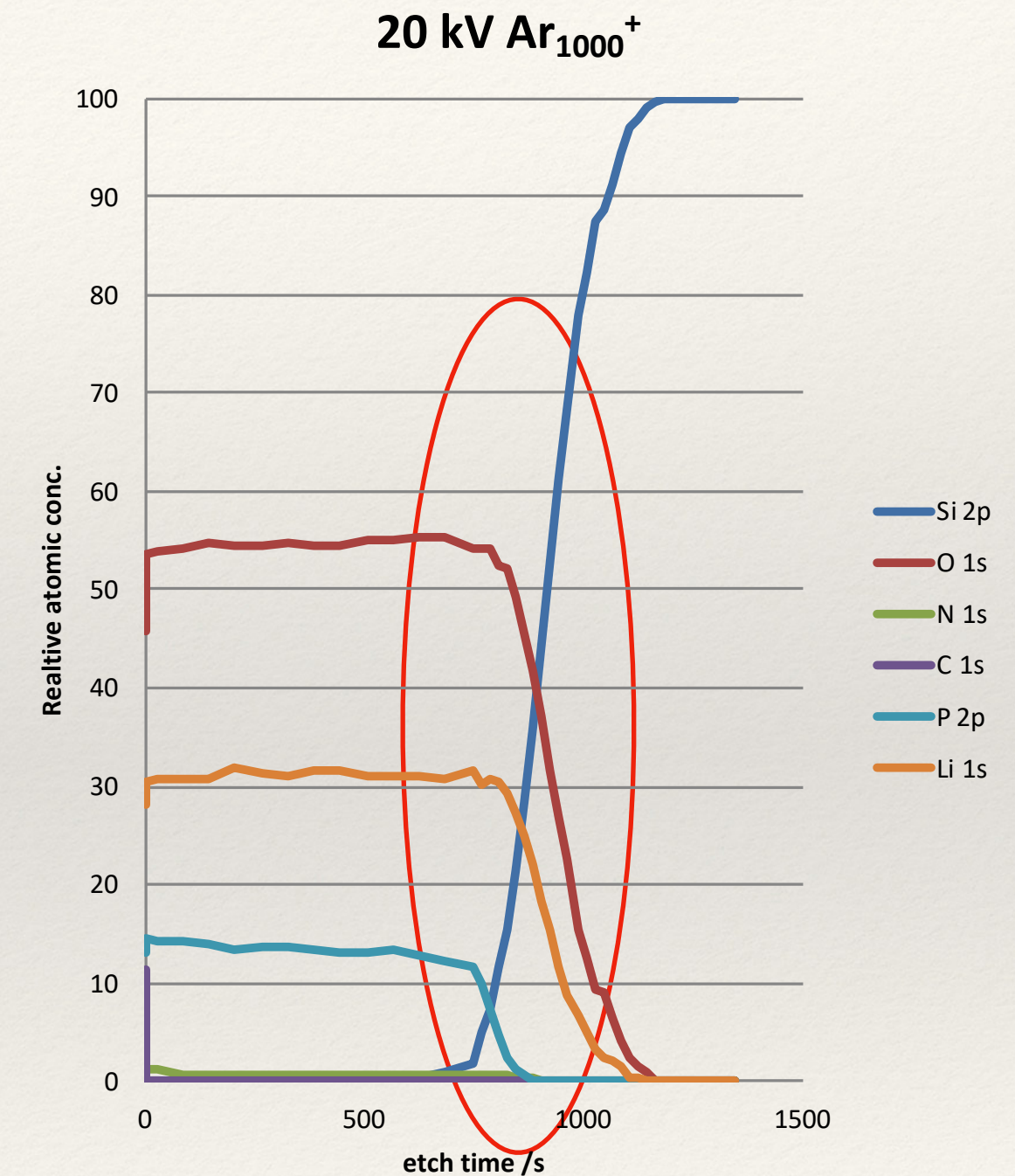


Sputtering with a Gas Cluster Ion Beam (/source): GCIB (/ GCIS)

Ar⁺ vs CGIB



Migration of Li under sputtering.
The chemistry is also affected



Mitigated migration of Li under sputtering.
The chemistry remains mostly unaffected

Ar+ vs CGIB

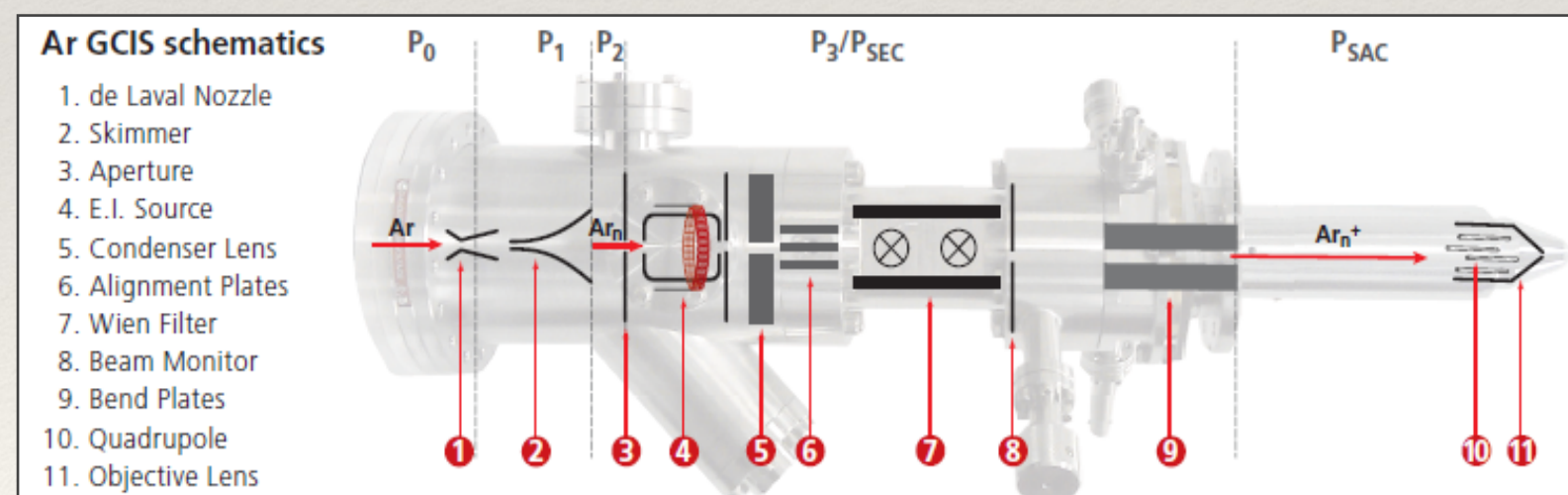
Ar+

- ❖ Easily calibrated sputtering rates
- ❖ Steady state in depth profile

- ❖ Preferential sputtering (ion beam induced oxides reduction) -> modification of the chemical structure
- ❖ Implantation

GCIB

- ❖ Excellent for surface cleaning of organics
- ❖ Mitigation of ion beam induced oxide reduction
- ❖ Lower relative level of preferential sputtering in organics. However, 'doesn't' sputter away metals!
- ❖ A lack of "steady state" is observed in gas cluster ion beam depth profiles



Schematics of Kratos GCIB

Further reading: R.Simpson et al. XPS investigation of monatomic and cluster argon ion sputtering of tantalum pentoxide. Applied Surf. Sci. 405, 2017



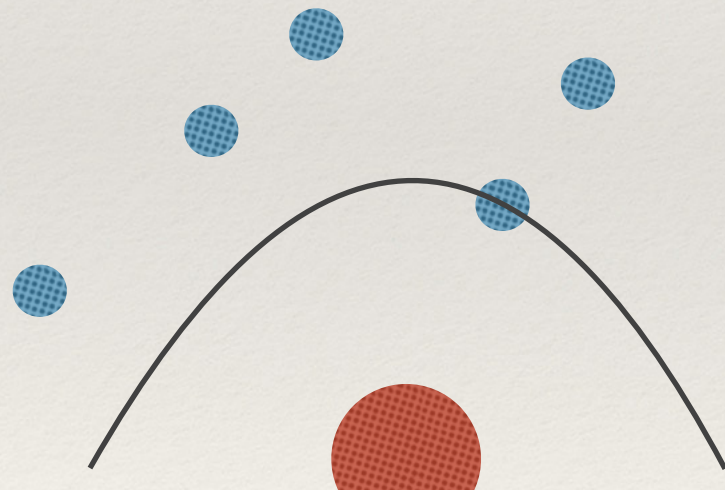
Istanbul Spices Market

‘Chemical Shift’

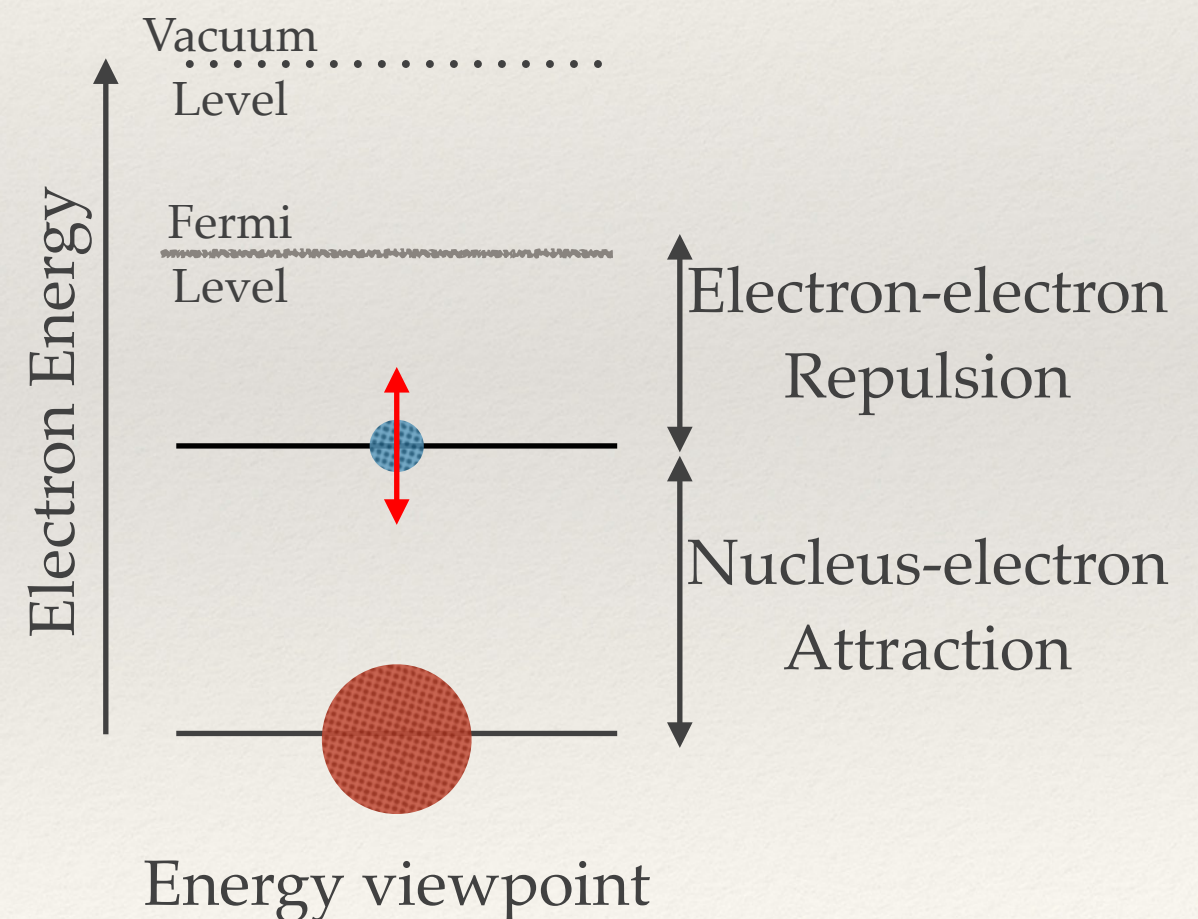
Origins and basic principle:
‘Flavours’ of an element

XPS 'vs' ESCA: Chemical Shift

- ❖ Initially called Electron Spectroscopy for Chemical Analysis (ECSA) by K. Siegbahn, XPS reveals its full potential due to the **chemical shift**, i.e. BE shift, arising from the displacement of electronic orbitals upon changes in the atomic charge distribution
- ❖ K. Siegbahn showed that the chemical shift is a linear function of the net charge transfert in chemical bounding

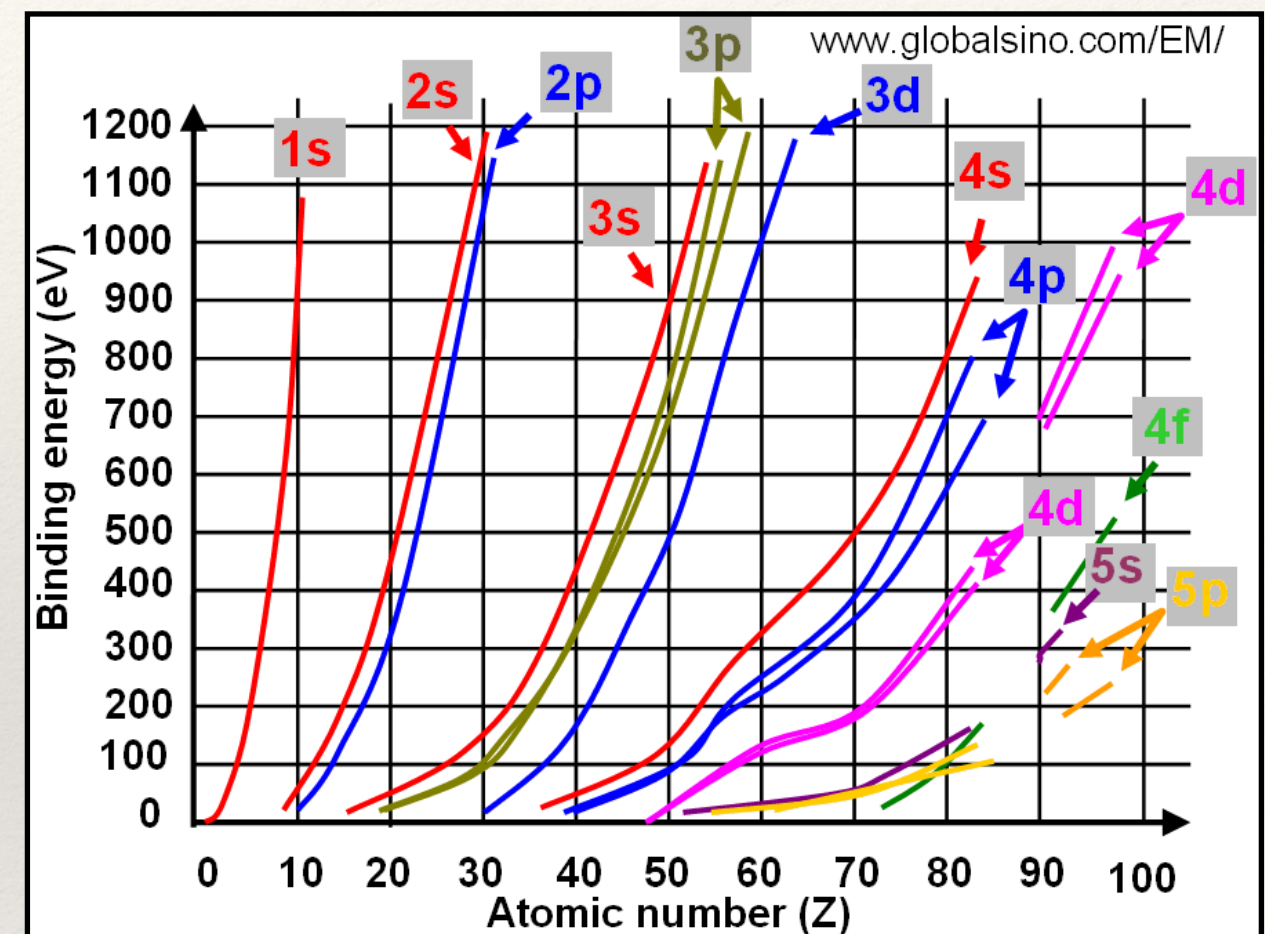


Atomic viewpoint



Binding Energy vs Z

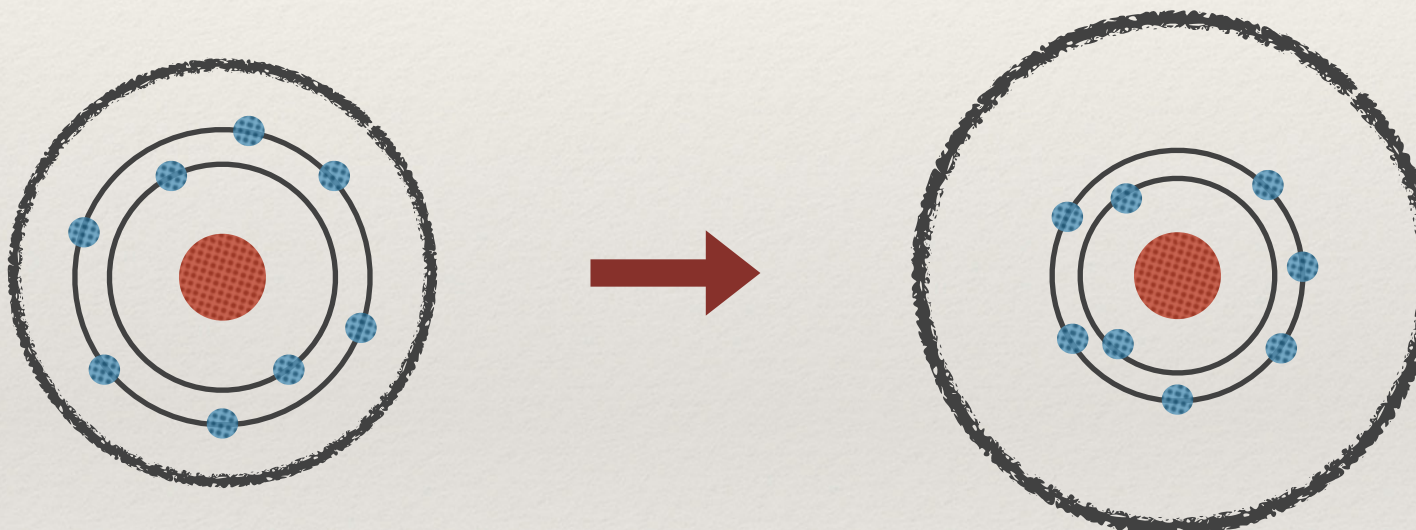
- ❖ Due to Coulombic attraction between the nucleus and the electronic orbitals, the BE increases with Z (for the same line of the periodic table)
- ❖ For the same reason the BE remains mostly unaffected by isotopes
- ❖ **But: Coulombic force is screened by valence electron, hence chemical shift**



Electron binding energy vs atomic number Z, for low binding energies

Binding Energy vs Electronegativity

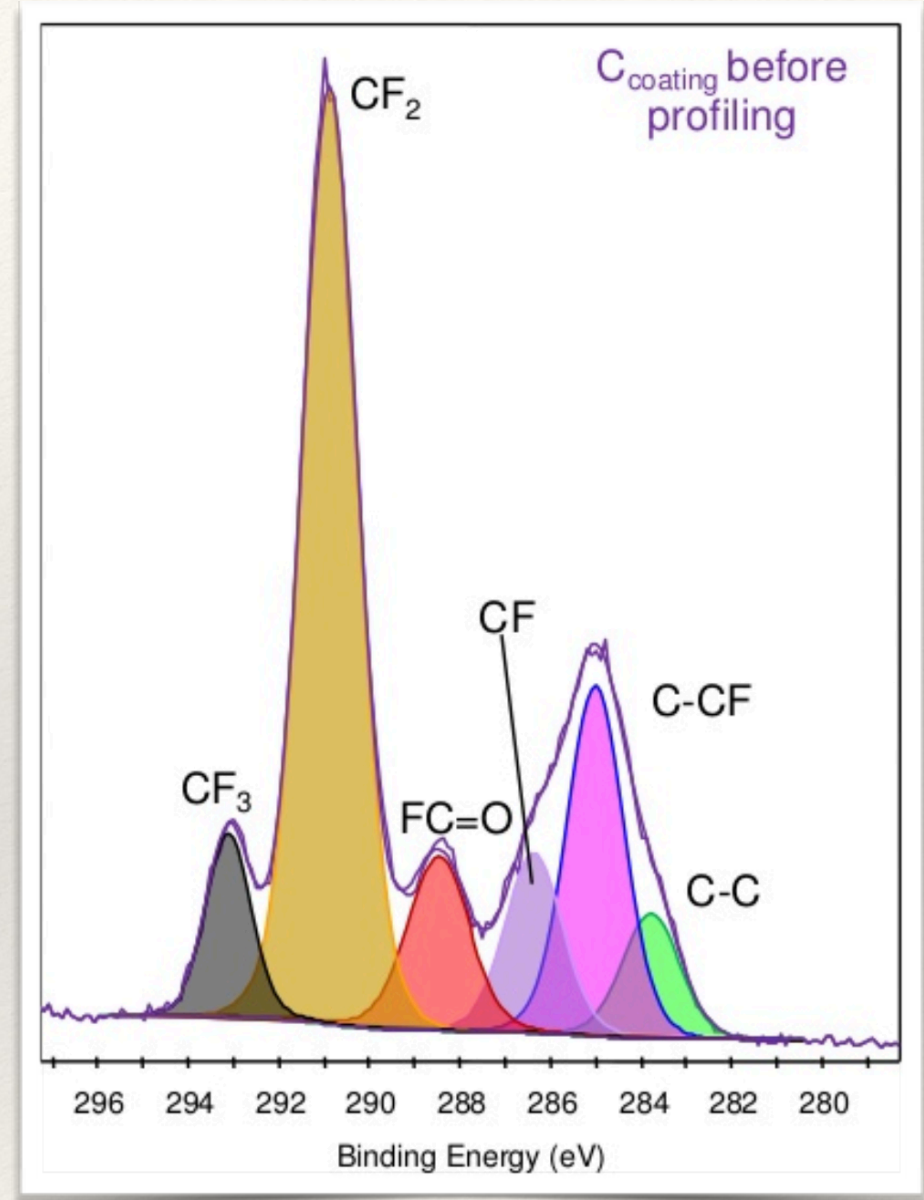
- When a covalent bond is created, electron density is increased at the more electronegative partner.
- The average radius of the valence band of the 'donor partner' increases
- Due to a decrease in the valence electrons screening, the core electrons are shifted towards the nucleus, and therefore increasing their binding energy, hence the 'chemical shift'



Group		BE eV	
hydrocarbon	C-H, C-C	284-285	
Amine	C-N	285.6	
Alcohol	C-O-H, C-O-C	286.5	
Cl bound	C-Cl	287.0	
F bound	C-F	287.8	
Carbonyl	C=O	288.0	Electronegativity

Chemical Shift and Bounding

- ❖ When a covalent bond is created, electron density is increased at the more electronegative partner.
- ❖ The average radius of the valence orbitals of the 'donor partner' increases
- ❖ Due to a decrease in the valence electrons screening, the core electrons are shifted towards the nucleus, and therefore increasing their binding energy, hence the 'chemical shift'

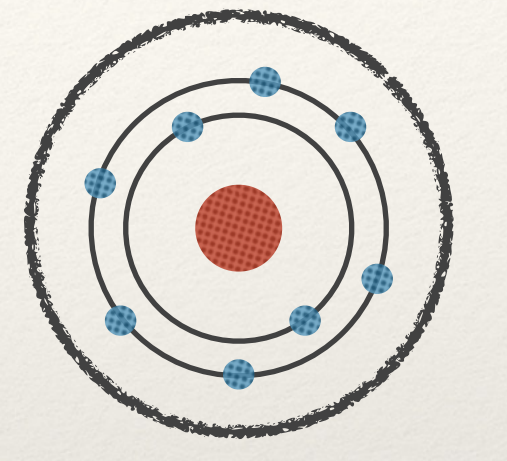


Source: Thermo-Fisher database

BE of a Free Atom

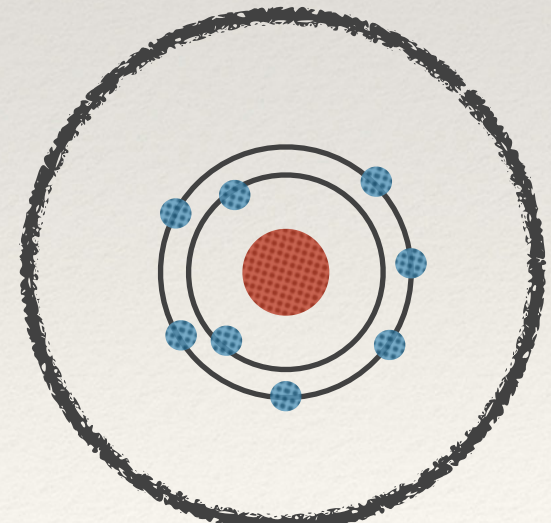
- ❖ Starting from the Koopman's 'frozen orbitals' theorem, i.e.: **BE = - Hartree-Fock energy**

$$E_b^v(j) = - \epsilon_{HF}(j)$$



- ❖ Let's include a change in the valence charge:

$$E_b^v(j) = - (\epsilon_{HF}(j) - V_{valence_shift})$$



BE in the Condensed Phase

Further terms have to be added to address:

- ❖ The intra-atomic relaxation energy
- ❖ The inclusion of our free atom in the condensed phase: Change in Hartree-Fock due to Madelung potential
- ❖ The extra-atomic relaxation energy (reaction of the surrounding atoms to the ionisation of the target atom)
- ❖ The work function

$$E_b^v(j) = -\epsilon_{HF} + V_{valence_shift} - R_{atomic} + V_{Madelung_shift} - R_{extra-atomic} - \phi$$

The Chemical Shift

From the previous equation, only part of the terms vary upon a modification of the chemical bounding and environment. The **chemical shift** might then be expressed as:

$$E_b^v(j) = -\epsilon_{HF} - R_{atomic} + V_{valence_shift} + V_{Madelung_shift} - R_{extra-atomic} - \phi$$

$$\Delta E_b^v(j) \cong \boxed{\Delta(V_{valence_shift} + V_{Madelung_shift}) - \Delta R_{extra-atomic}}$$

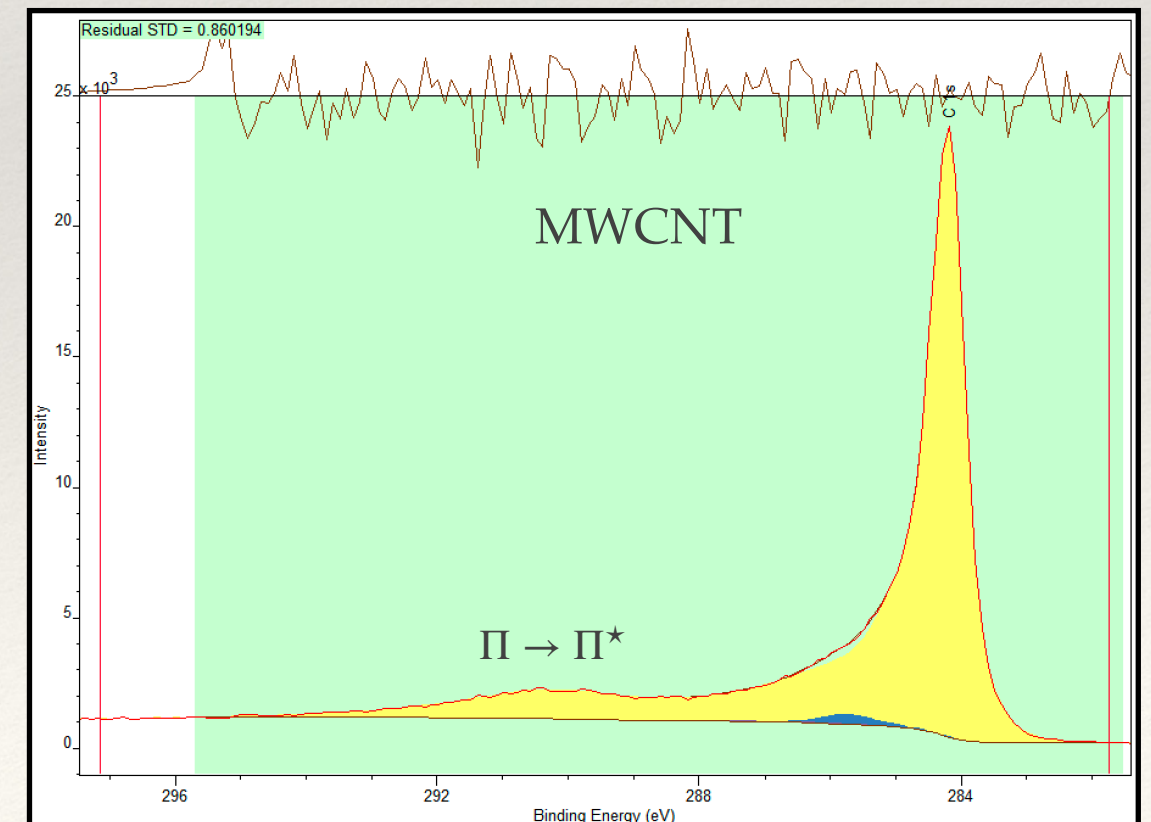
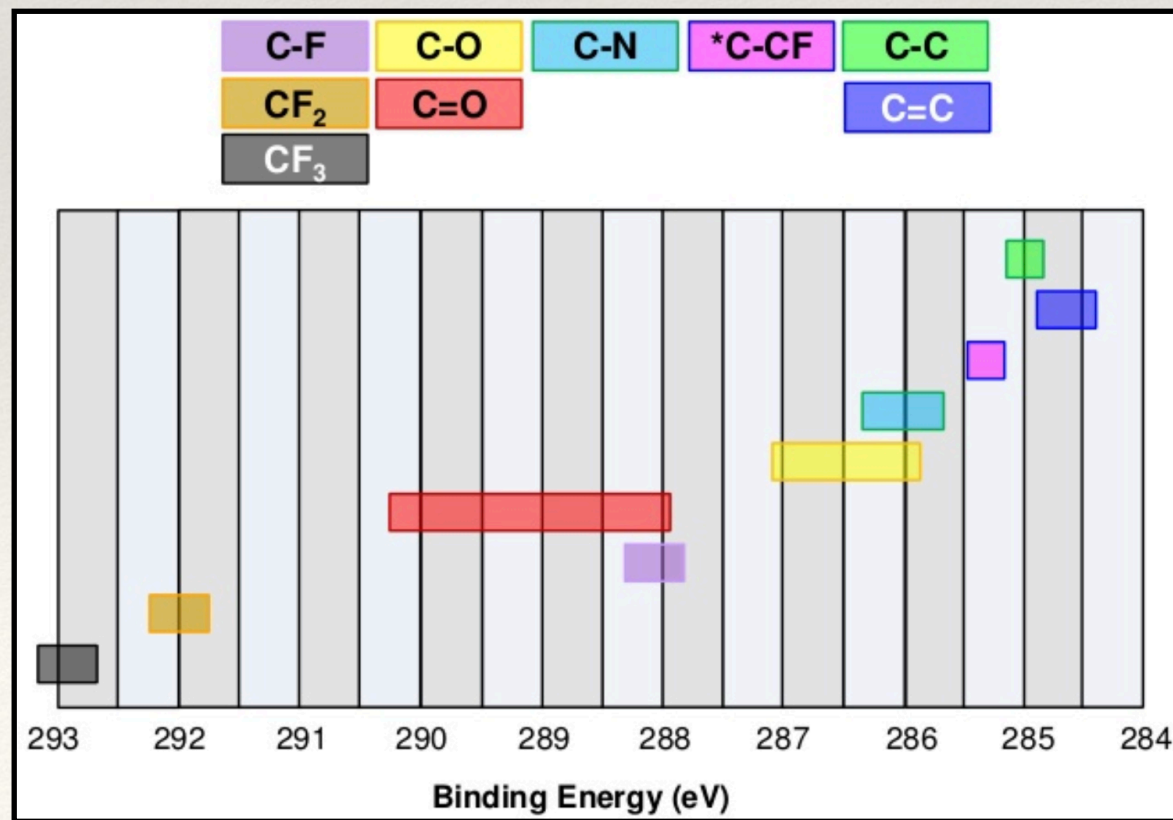
$\propto -\Delta q/r \quad \propto -\alpha \Delta q/r$

Electronegativity

Polarizability

Typical Chemical Shift

- ❖ Different chemical bounds might be distinguished! But not always: overlaps are often present, e.g. $BE_{C-N} \cong BE_{C-O}$
- ❖ Chemical shift reaches up to 15eV
- ❖ Hybridization induces chemical shift, although with a mild intensity
- ❖ $\Pi \rightarrow \Pi^*$ appears at ~ 290 eV



Quantitative XPS: PE Cross Section

- ❖ When two particles interact, their mutual cross section is the area transverse to their relative motion within which they must meet in order to scatter from each other.
- ❖ The optical excitation cross section $\sigma(E)$ in a subshell nl is given by:

$$\sigma_{n,l}(E) = \frac{4}{3}\pi^2 a_0^2 \left\{ \alpha [N_{n,l}[E - E_{n,l}] \frac{1}{2l+1} \right\} [lR_{E,l-1}^2 + (l+1)R^2 - E, l+1]$$

Where n, l : quantum numbers, α : fine structure constant, a_0 : Bohr radius, N ...

...Finally, after some calculations:

$$I(\theta) \propto \frac{\sigma_{tot}}{4} \left[1 - \frac{\beta}{4\pi} (3 \cos \theta - 1) \right]$$

where β is the asymmetry parameter, θ the take-off angle, σ_{tot} the total cross-section

Quantitative XPS

The surface area of the peaks contain the information about the so-called, **relative surface atomic concentration, at%**

The intensity of a peak j of an element i is described by I_{ij} :

$$I_{ij} = n_i K T(KE) \sigma_{ij} \lambda(KE) \cos(\theta)$$

Atomic concentration of i
Transmission function of the constant
Instrument function of the analyser
Photoionization cross-section
IMFP
Emission angle

Quantitative XPS

The relative surface atomic concentration C_i of an element i is therefore equal to:

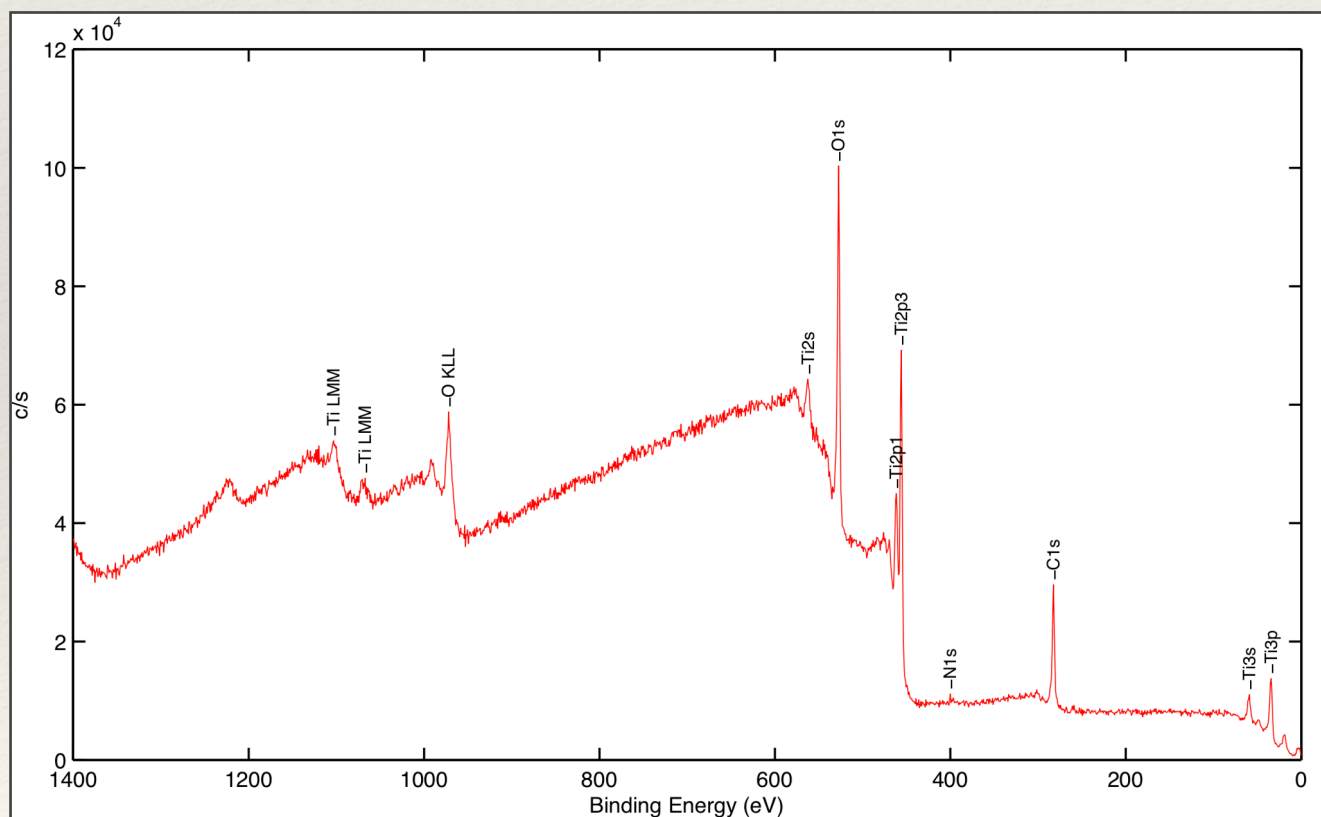
$$C_i = \frac{I_{ij}/\sigma_{ij}\lambda(KE)}{\sum I_{ij}/\sigma_{ij}\lambda(KE)} = \frac{I_{ij}/S_{ij}}{\sum I_{ij}/S_{ij}}$$

With $S_{ij} = \sigma_{ij}\lambda(KE)$, the relative sensitivity factor (RSF) of the transition j of element I .

Depending on the element, XPS sensitivity is about 0.1 at%

Study case II: TiO₂ Coating

A TiO₂ coating was measured without pre-sputtering, i.e., the surface is 'as received'. Here is the survey spectrum:



Survey spectra showing C, O, Ti, and possibly Na

In case of doubts check databases:
<https://xpssimplified.com/elements/titanium.php>

Photoelectron Lines				
2s	2p _{1/2}	2p _{3/2}	3s	3p
561	460	454	59	33
Auger Lines				
LM ₂₃ M ₂₃		L ₃ M ₂₃ M ₄₅ (¹ P)		
1098		1068	(Al)	
		865		835 (Mg)

Study case II: TiO₂ Coating

Given the peak area and the relative sensitivity factor, evaluate the surface atomic concentration of the different elements composing the surface:

	Area	RSF
C 1s	17400	0.314
O 1s	54570	0.733
Ti 2p	59855	2.077
Na1s	~0	1.102

$$C_i = \frac{I_{ij}/\sigma_{ij}\lambda(KE)}{\sum I_{ij}/\sigma_{ij}\lambda(KE)} = \frac{I_{ij}/S_{ij}}{\sum I_{ij}/S_{ij}}$$

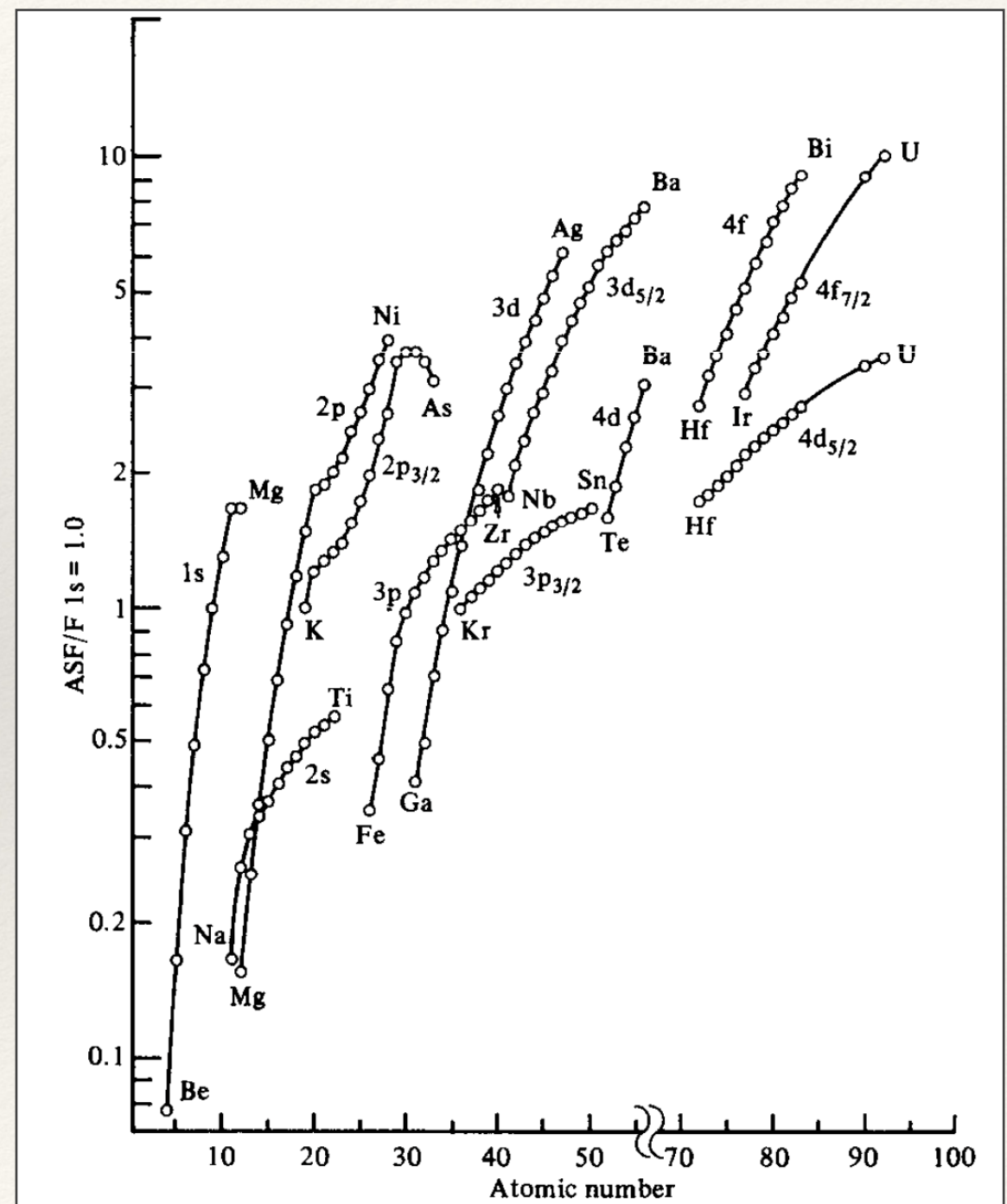
Study Case II: TiO₂ Coating

Given the peak area and the relative sensitivity factor, evaluate the surface atomic concentration of the different elements composing the surface:

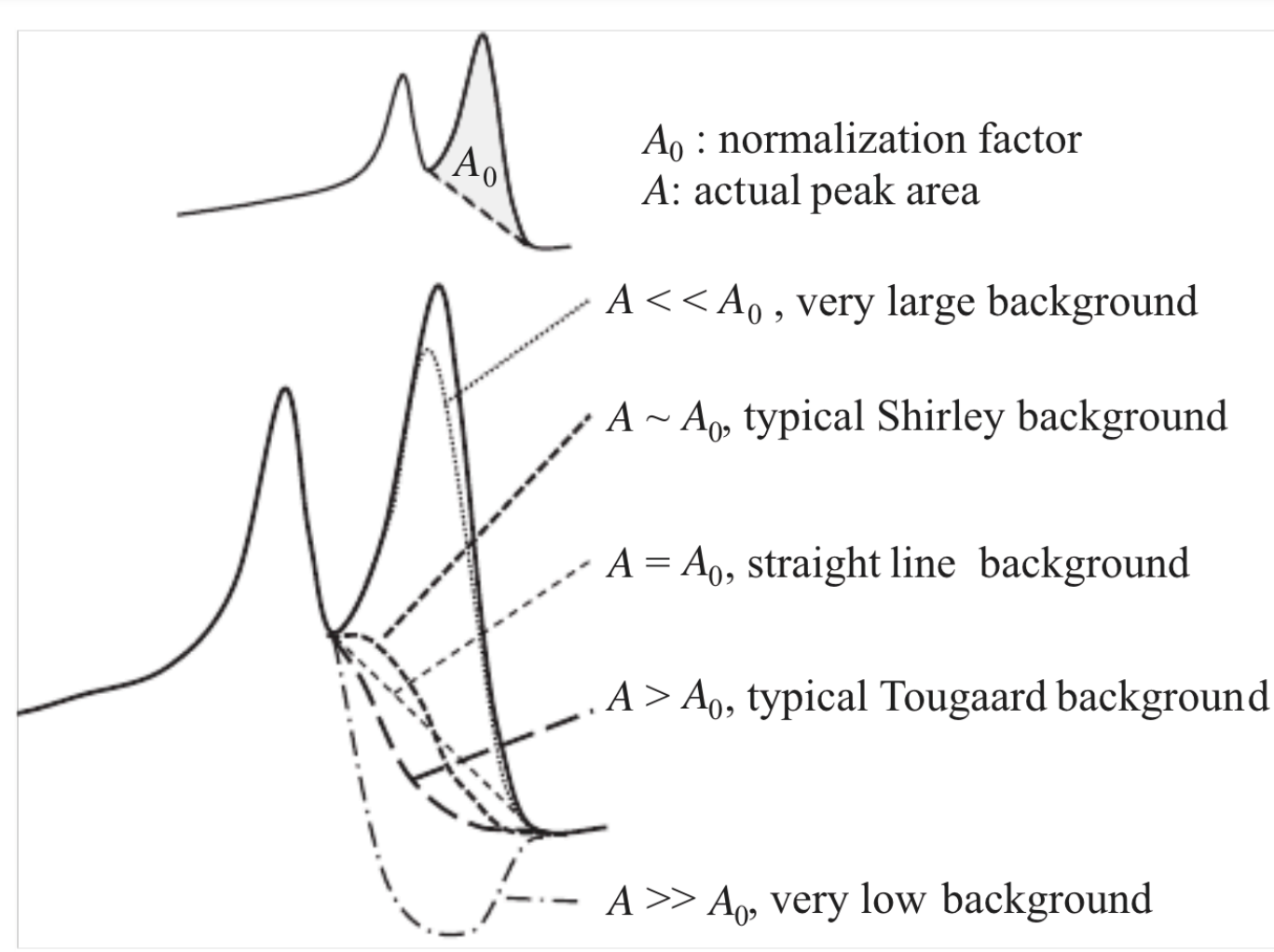
	Area	RSF	I/RSF	at%
C	17400	0.314	55414	34.9
O	54570	0.733	74458	46.9
Ti	59855	2.077	28818	18.2
Na	~0	1.102	0	0
Sum			158690	

Trends in PE intensities

- ❖ Importantly: the intensity of the PE tend to increase with the atomic number, and decrease towards the core orbitals. The orbital having the largest RSF is generally prioritised
- ❖ However: chemical shift might not necessarily be the largest for the orbital with the largest RSF, and / or other complications such has overlap, complex peak-shape might hinder the chemical analysis for a specific orbital
- ❖ Maximum information is often obtained by measuring Auger and PE lines of the same element

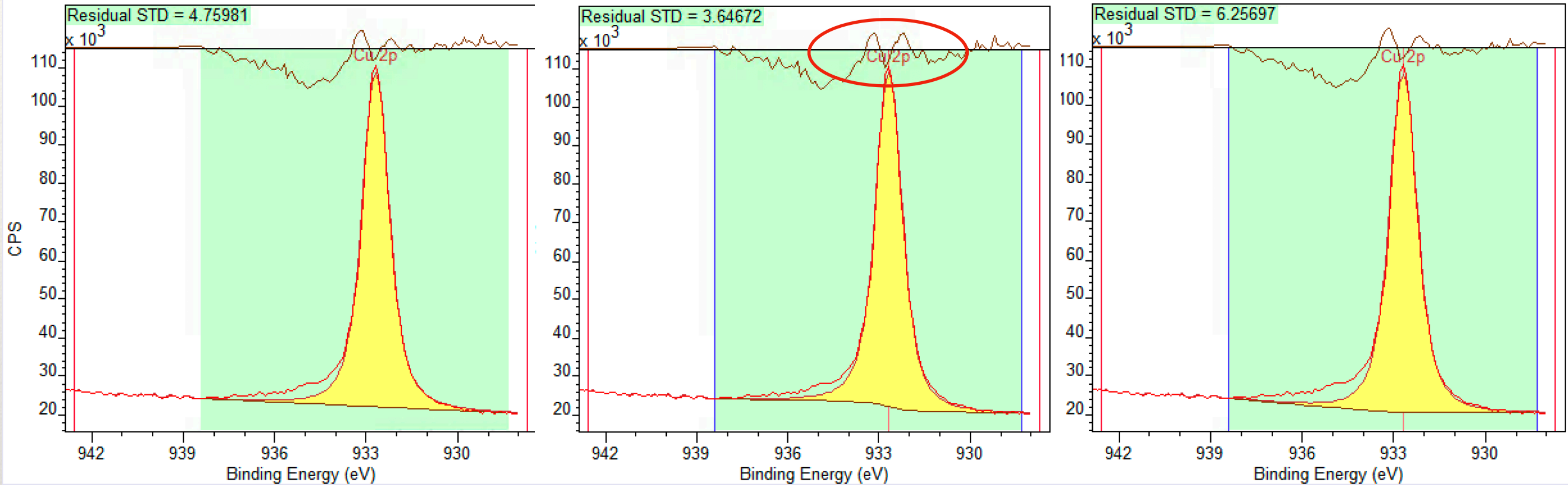


Regions for Quantification



- ❖ Several types of background (semi-empirical) exist. From the simplest linear background to iterative backgrounds such as iterative Shirley background.
- ❖ Conventional background are Shirley and Tougaard
- ❖ Iterative Shirley might not converge

Background: Symmetry of the Residuals



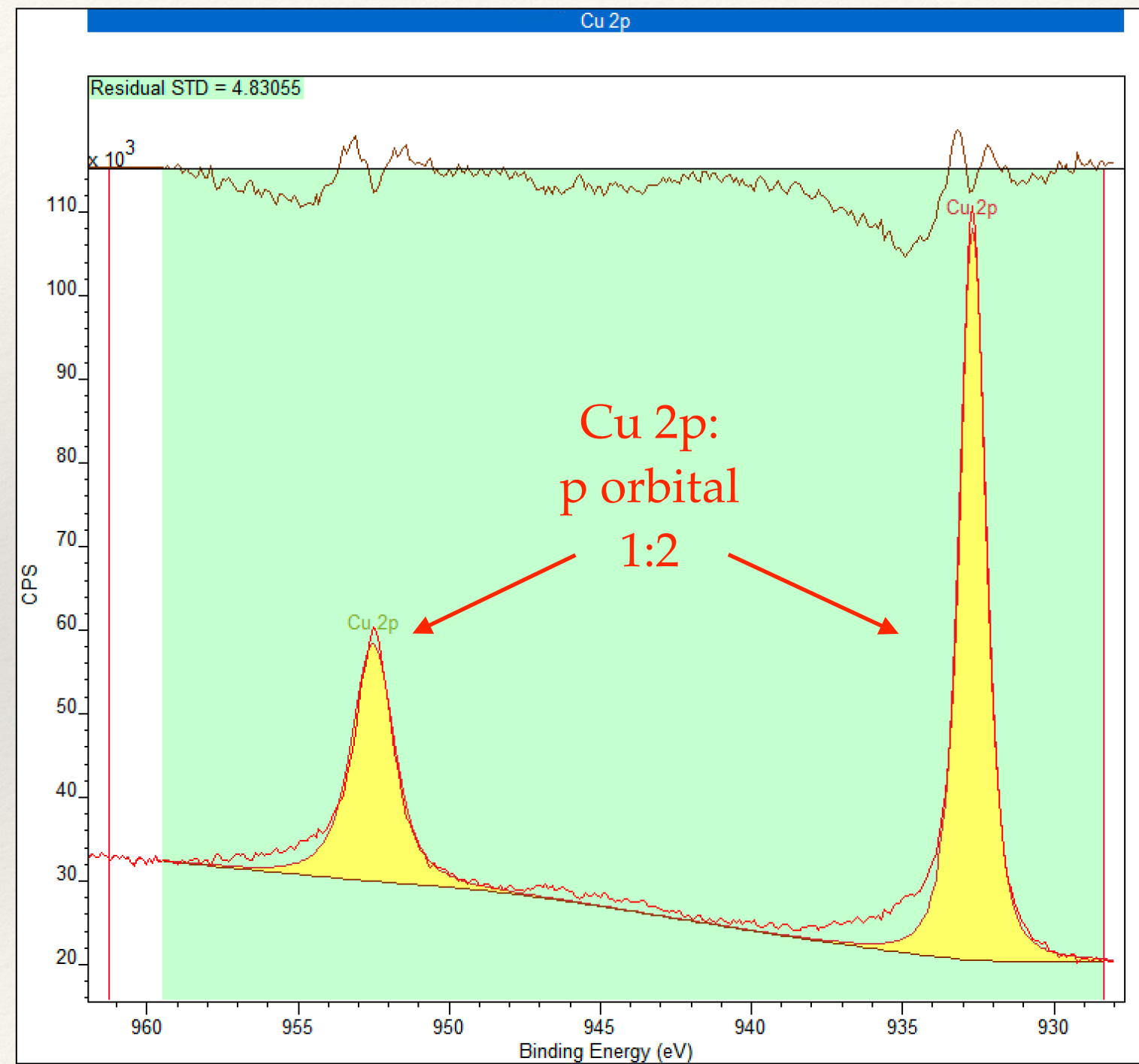
Typically, three types of backgrounds are used:

- ❖ Linear background (left)
- ❖ 'Shirley' background (middle) (intensity is proportional to the intensity of the total peak area above)
- ❖ Tougaard background (right) which integrates the intensity of the background at a given binding energy from the spectral intensities to higher kinetic energies

Background: Area Ratio

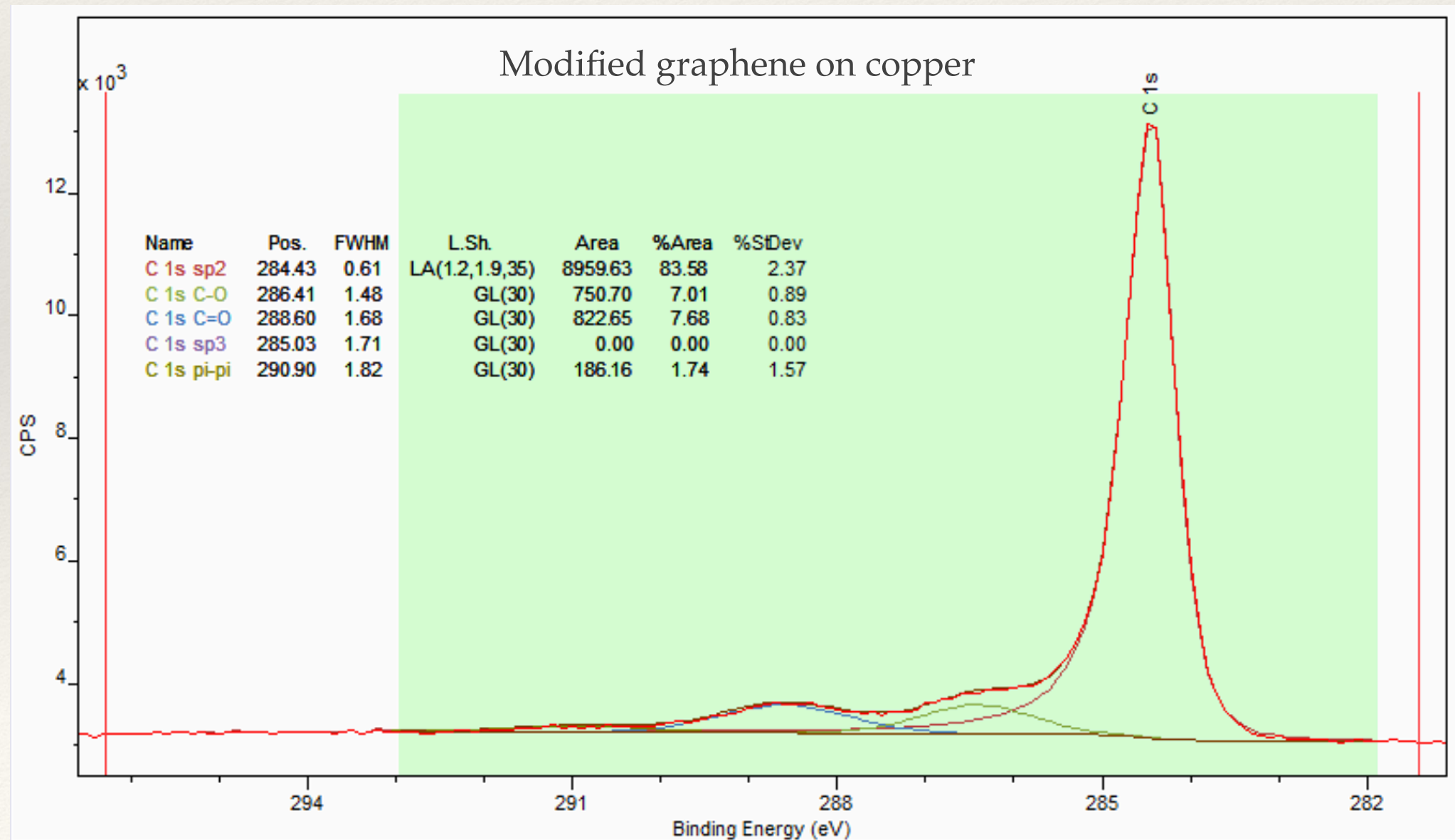
- ❖ Should never overlap the baseline
- ❖ Should reflect the expected lineshape: symmetric or asymmetric
- ❖ Should reflect the area ratio of the spin orbit splitting:

Subshell	j values	Area Ratio
s	1/2	n/a
p	1/2 3/2	1:2
d	3/2 5/2	2:3
f	5/2 7/2	3:4



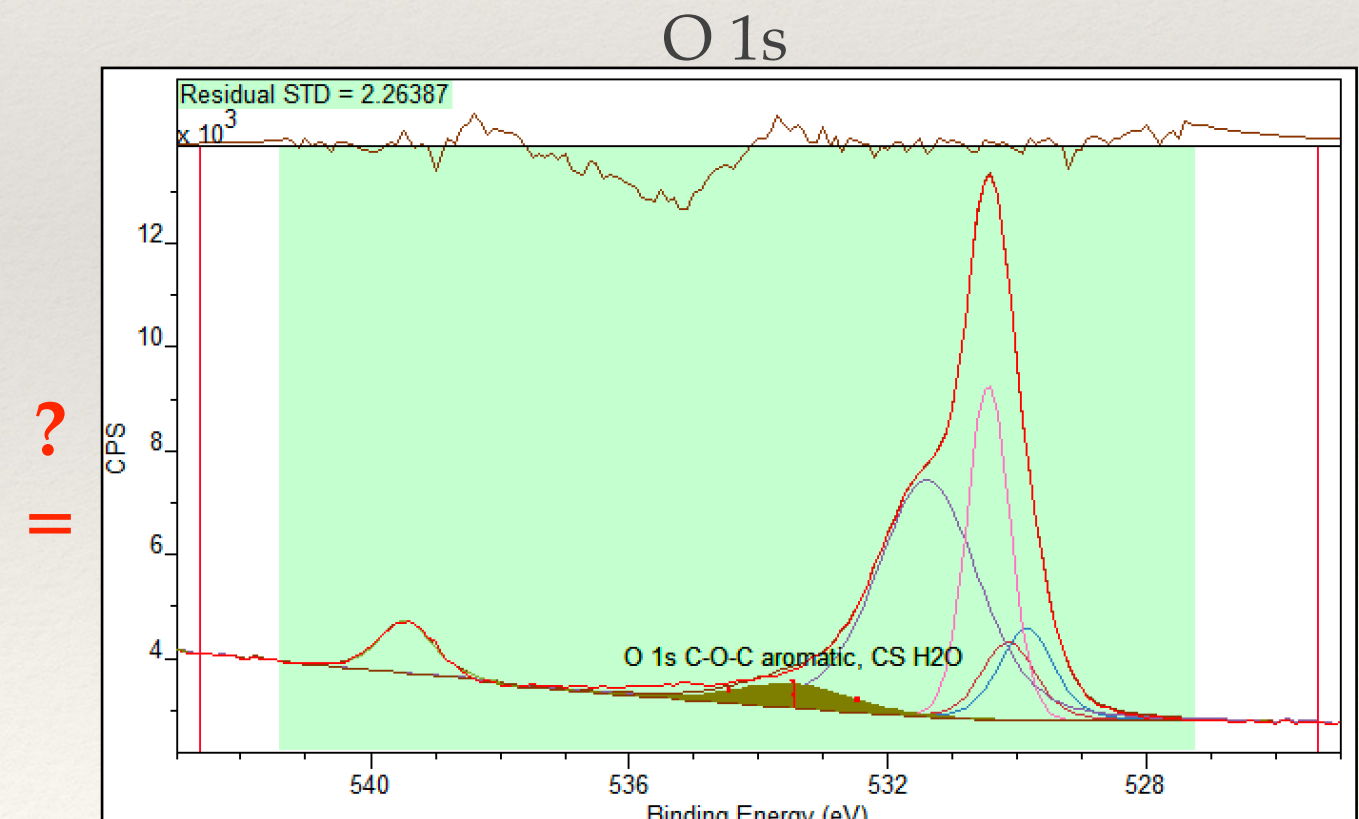
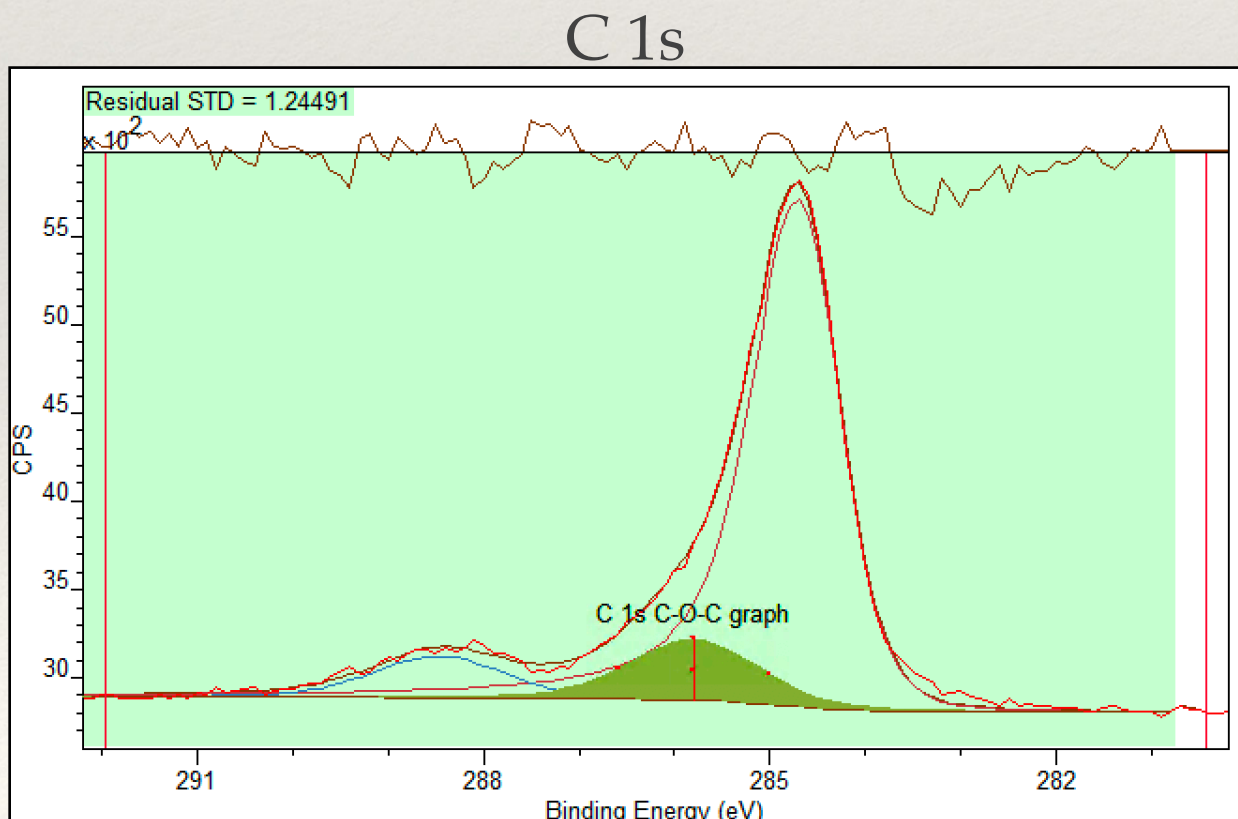
Components for Quantification

- ❖ Peak fitting present challenges: good references are compulsory, DFT can help
- ❖ Physico-chemical nature of the sample has to be considered, eg. spin-splitting!
- ❖ Statistics are useful...Monte Carlo simulations allow to assess the stability of the chosen peak model. In the next slides



Peak Fitting: Using Correlation

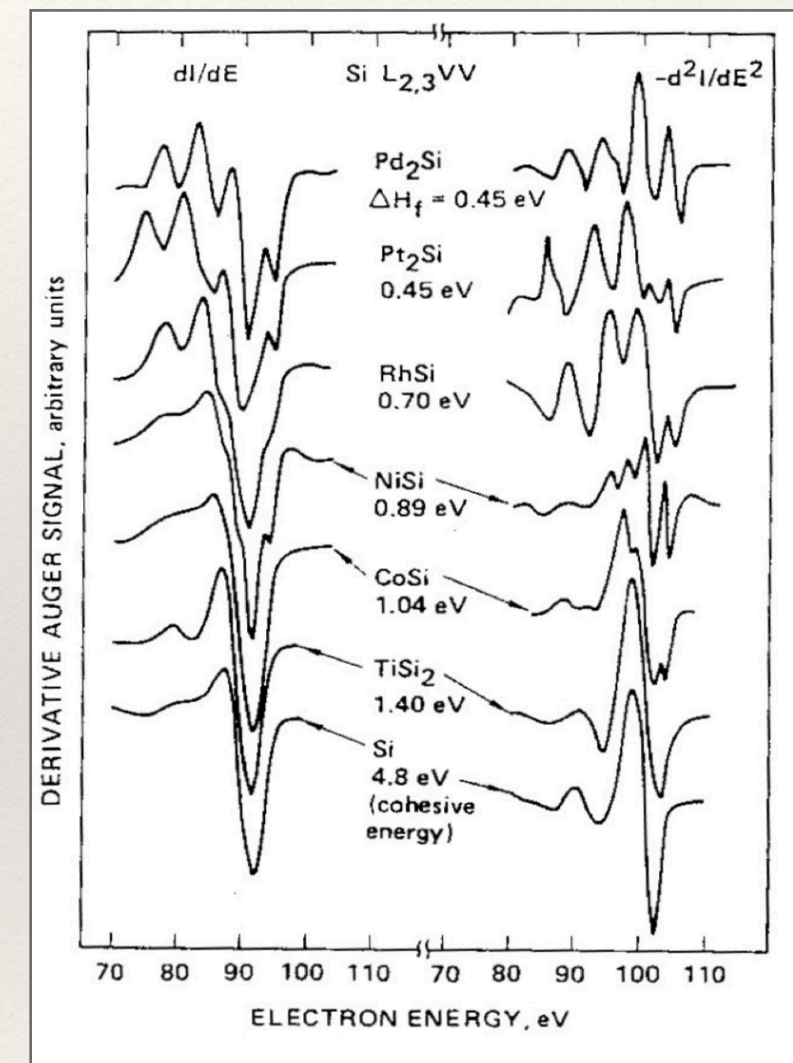
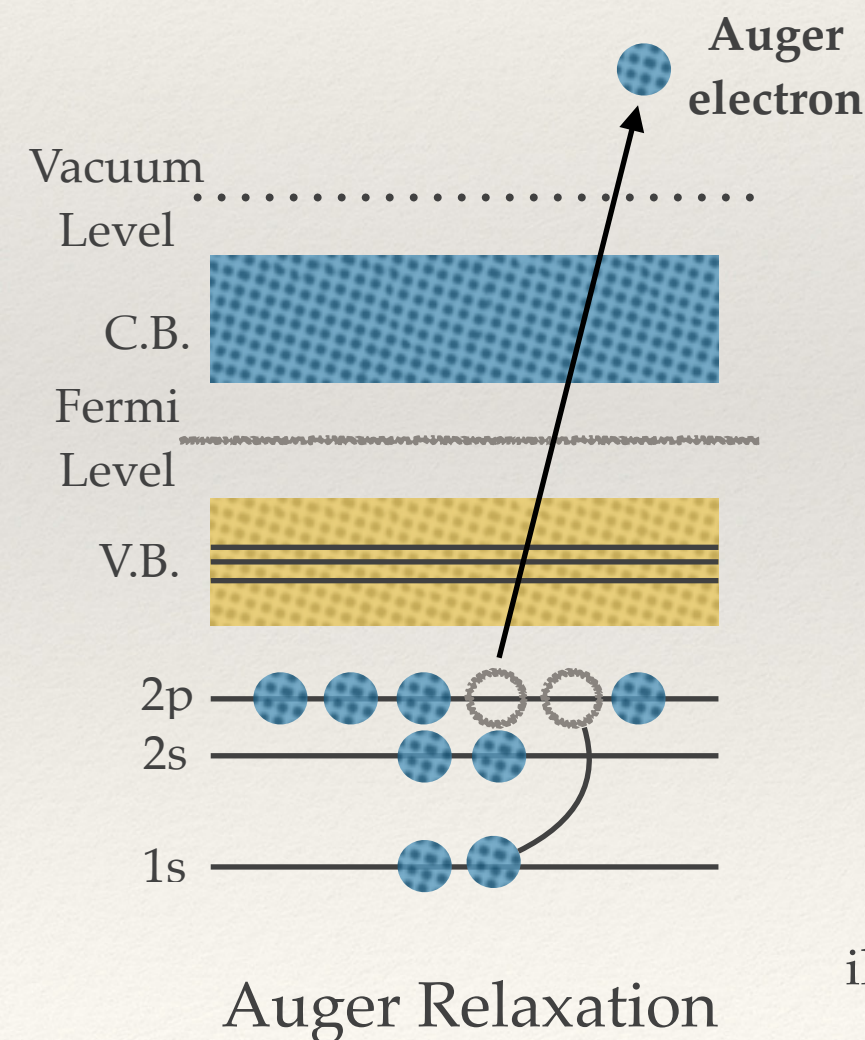
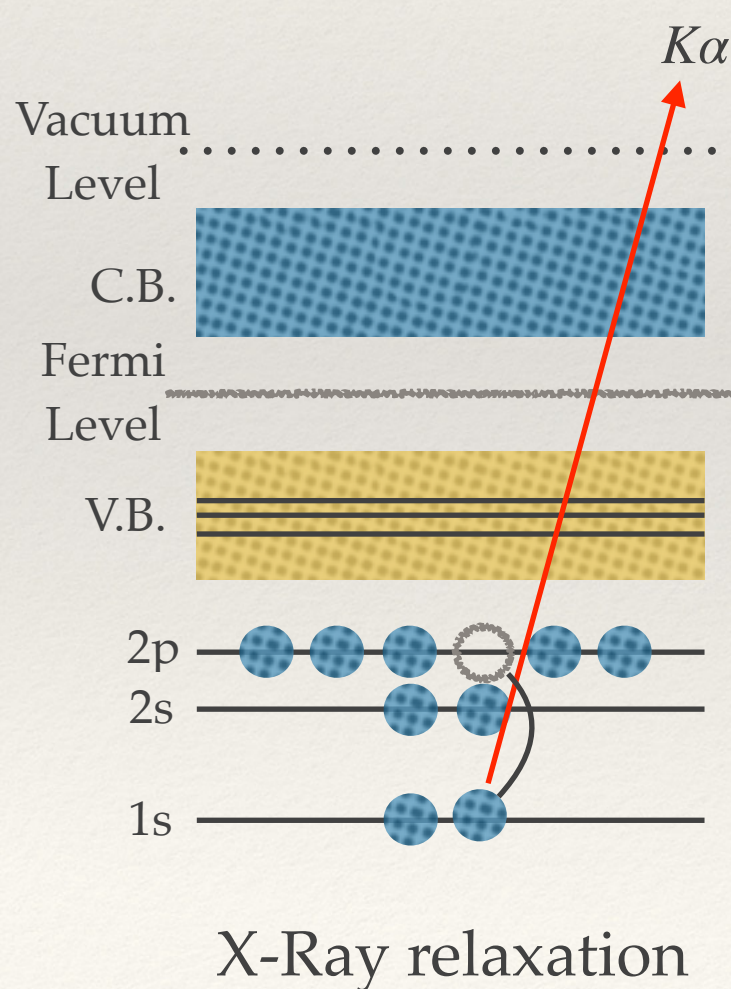
- ❖ Full understanding of the sample composition can only be obtained using the information provided, not only by the analysis of the photoelectron lines of all the elements presents, but also the Auger spectra, and background
- ❖ Chemical state analysis should be coherent between the different orbital of pairwise chemical bounds, e.g. **C-O as measured on C 1s should relate to C-O as measured on O 1s**



Relaxation Paths

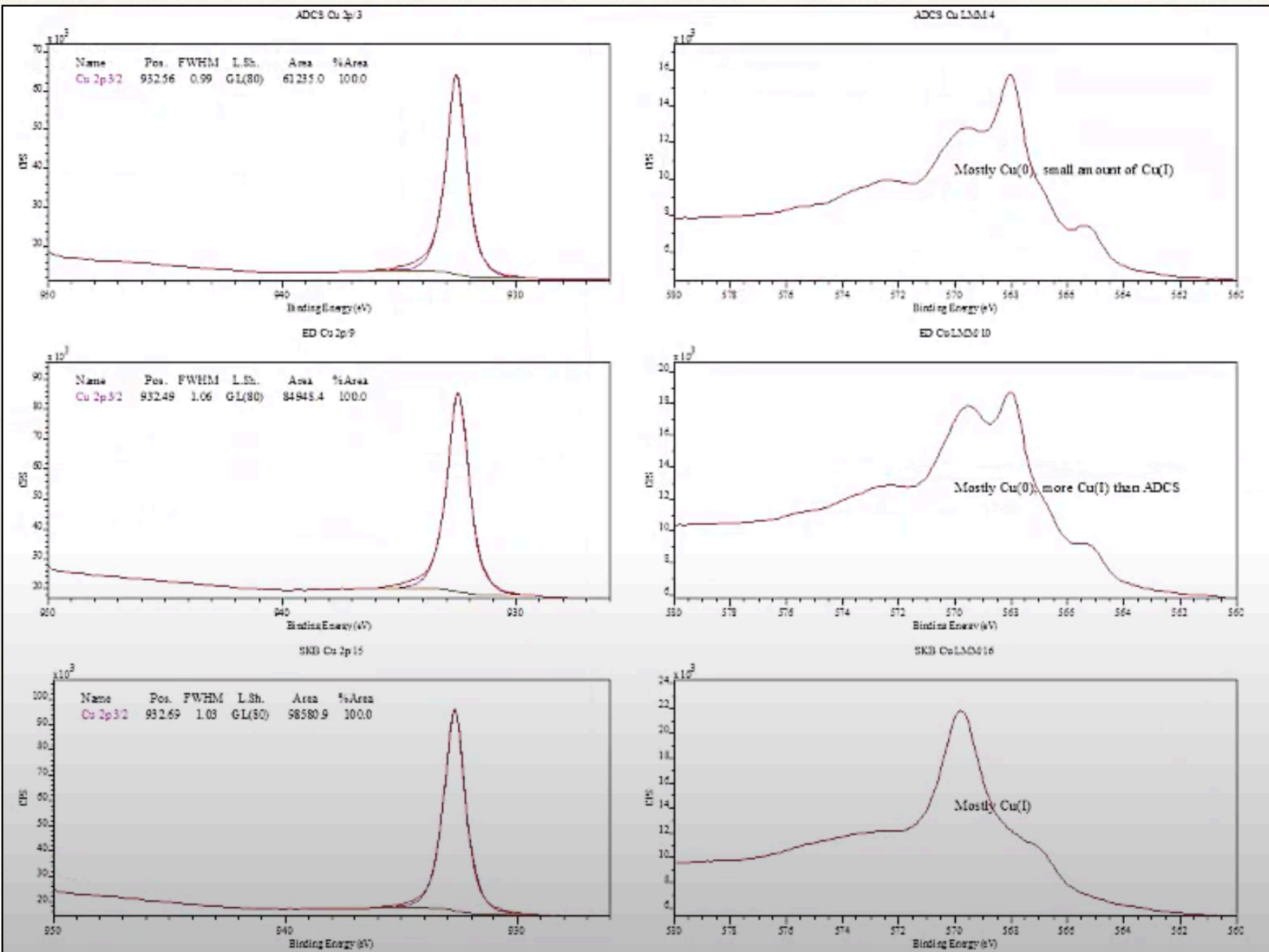
Auger electron emission is a 3 electrons phenomenon. In a KLL transition, from a K level vacancy created from the emission of a photoelectron (middle)

- ❖ L level electron fills the K level vacancy
- ❖ The energy is transferred to a L level Auger e-



First and second derivatives of AES spectrum for different silicides, illustrating the complexity and richness of the spectral feature. Source: Scudiero.

The Importance of Auger Electrons



Used in combination with photoelectron analysis, Auger electron might provide a great help in understanding the exact nature of a sample.

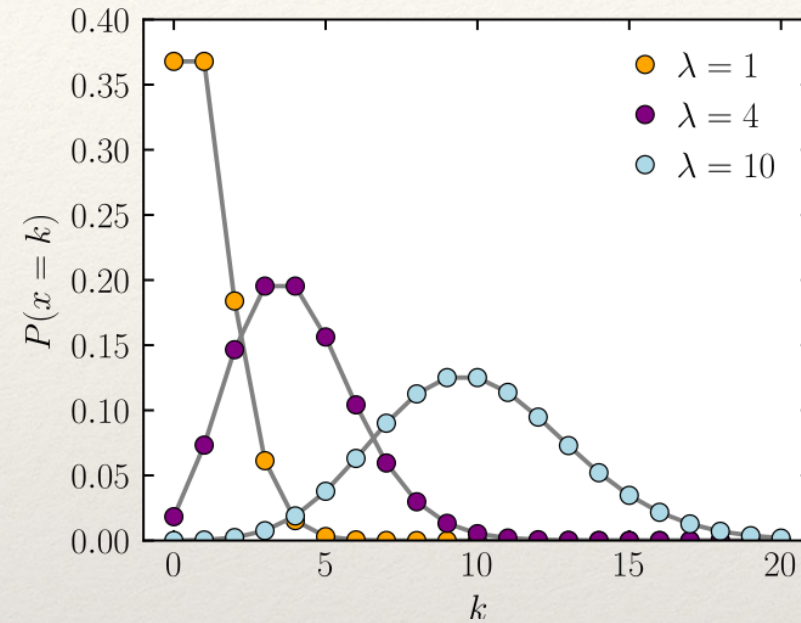
For copper:

The so-called Auger parameter allows to distinguish between Cu(I) and Cu(II), but also between

Fitting Cu LMM further allows to distinguish between CuO and Cu(OH)2

Peak Model: Stability Test

XPS measurements are subject to noise in the form of Poisson distribution



Reducing noise is not always possible as statistics plays against us as:

$$\bar{x} - q(\cdot \%) \frac{\sigma}{\sqrt{n}} \leq \mu \leq \bar{x} + q(\cdot \%) \frac{\sigma}{\sqrt{n}}$$

- Sample degradation under X-ray exposure limits acquisition time
- Repeating an experiment many times is not practical

Noise Estimation:

http://www.casaxps.com/help_manual/casaxps2316_manual/error_estimates_in_casaxps.pdf

Monte-Carlo Simulation

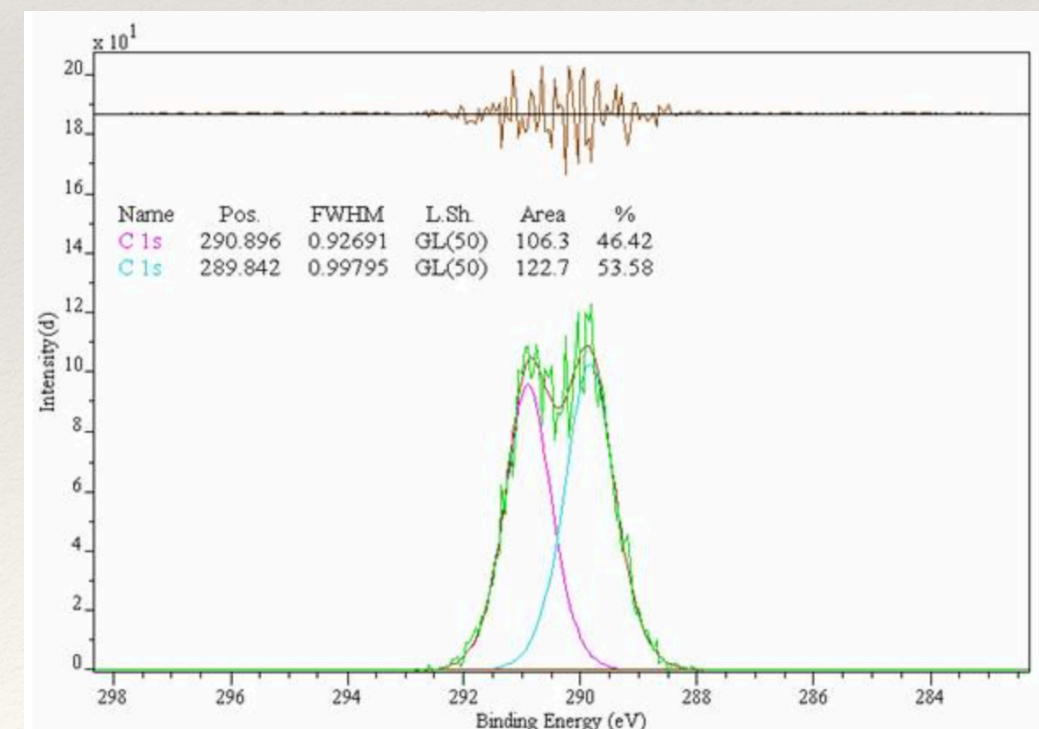
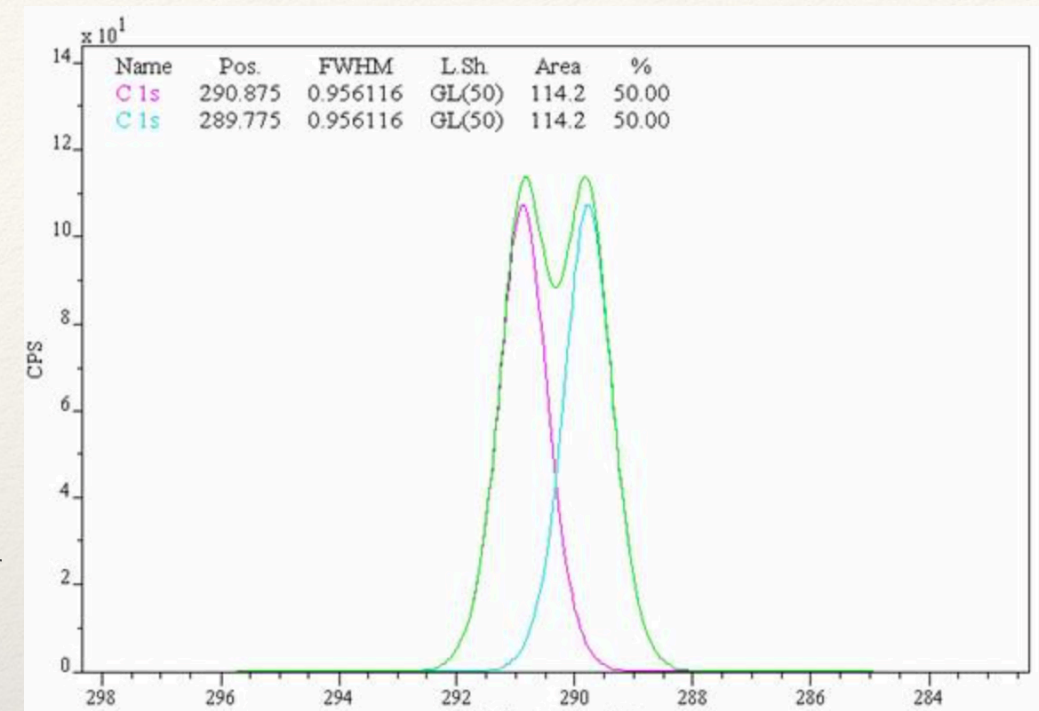
A large data set might be generated from a single measurement, by:

- Removing the noise of the measured data
- Adding Poisson noise to the de-noised data

This data set might then be fitted using a peak model to test its stability.

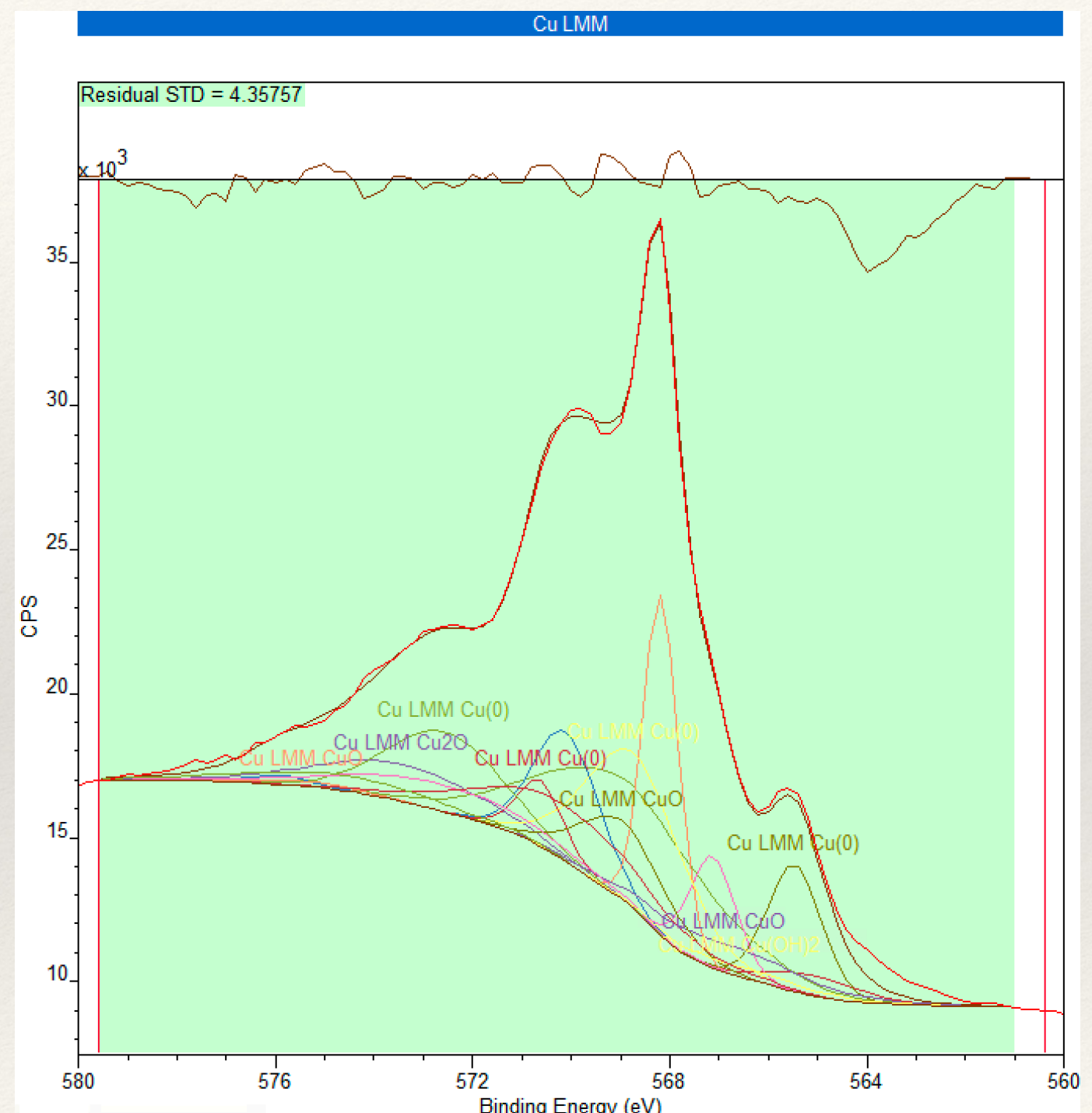
The parameters of the fitting indicate the sensitivity of the model to noise. This is of particular importance for 'noisy' data, e.g. measurements on monolayer, contaminants, etc

Monte Carlo Simulation: More information and figures from:
http://www.casaxps.com/help_manual/error_analysis.htm



XPS Fitting Guidelines

- ❖ Use well defined function matching the physical properties of your sample, e.g. Gaussian-Loretzian, assymmetric, etc.
- ❖ Use reference materials to calibrate your system
- ❖ Don't forget the spin splitting properties
- ❖ When possible, use Auger parameters
- ❖ Always cross correlate: C1s -> O1s, C1s



A well tested and trustworthy model is crucial to be able to rely on similar fitting

Summary

- ❖ Sputtering and depth probing, are useful at removing contaminants and probing at depth, however, the technique inherently brings several undesired effects
- ❖ Chemical shift analysis allows the evaluation of the chemical state of the measured elements
- ❖ XPS quantification has a typical sensitivity limit of ~0.1at%. RSF tables are used to make our life easier: no heavy calculation!
- ❖ Dedicated technique might prove very useful alternatives when the right conditions are met: ARXPS requires a layer of <10nm to be effective

Thank you!

Next course

- ❖ UPS
- ❖ XPS live example
- ❖ Auger Electron Spectroscopy
- ❖ Intermolecular forces: Introduction
- ❖ Scanning Probe Microscopy (SPM)
 - ❖ Scanning Tunneling Microscopy (STM)
 - ❖ Atomic Force Microscopy (AFM)

References

- ❖ Briggs et al. *Practical surface analysis*, Wiley, 1990
- ❖ L.E. Davis, *Handbook of Auger Electron Spectroscopy*. Perkin-Elmer, 1976
- ❖ Thermo-Fisher XPS webpage:
<https://xpssimplified.com/whatisxps.php>

Gloves case: <http://www.revbase.com/tt/sl.ashx?z=73090c66&dataid=433139&ft=1>